AD707720

STUDY OF ILLUMINATING FLAMES FROM SOLID REACTANTS

CLEARINGHOUSE

PREPARED BY

RESEARCH AND DEVELOPMENT DEPARTMENT

NAVAL AMMUNITION DEPOT, CRANE, INDIANA

D D C
RECEIVED
JUN 26 1970
C

DISCLAIMER NOTICE
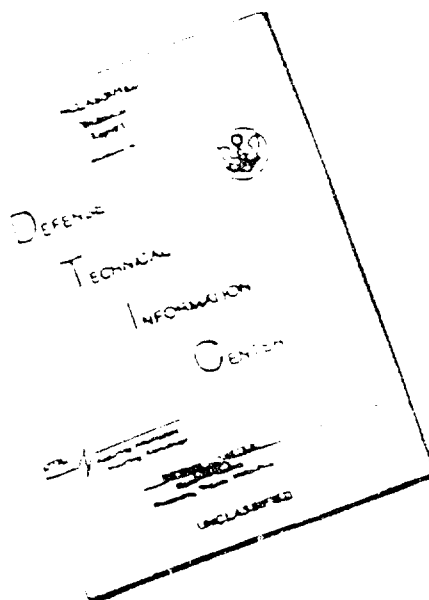
NAVAL AMMUNITION DEPOT
Crane, Indiana 47522

RDTR No. 77
1 June 1970

STUDY OF ILLUMINATING
FLAMES FROM SOLID REACTANTS

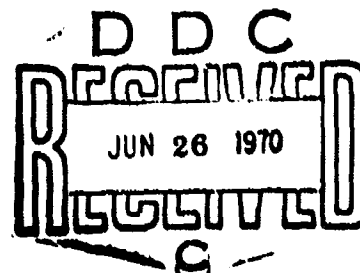R. M. Blunt
Denver Research Institute

!

This report was reviewed for adequacy and technical accuracy
by B. E. Douda.

Released

B. H. Calkins (signature)

B. H. CALKINS, Manager
Concept Development Division
Research and Development Department

Final Report 4178-7003-F

STUDY OF ILLUMINATING
FLAMES FROM SOLID REACTANTS

Final Report
1 August 1968 - 1 April 1970

by
R. M. Blunt

FOREWORD

This report summarizes and describes the work done on Contract N00164-69-C-0036 during the period from 1 August, 1968 to 1 April, 1970.

During this time many good discussions of the problems studied have been held with Mr. B. E. Douda of the U.S. Naval Ammunition Depot, Crane, Indiana. Thanks are due Mrs. Jeanne Tucker and Mrs. Bernice Bender, Computer Services Division, Environmental Science Services Administration, Research Laboratory for their help in the reduction of the data. Mr. Donald Dubbert and Mr. Marshall Parker of the Electronics Division, Denver Research Institute, were instrumental in establishing the foundation for the data reduction procedures which were finalized at ESSA, while Mr. George Crater and Mr. Ole Thompson have contributed greatly to the successful completion of the experimental work.

i

TABLE OF CONTENTS

LIST OF TABLES

LIST OF FIGURES

APPENDICES

    A. Alkali & Alkaline Earth Spectral Intensity
       Plots of the 0.43 micron to 1.17 micron
       Region

    B. Alkali & Alkaline Earth Flame Spectra
       from 0.35 micron to 0.90 micron

    C. Detailed Tabulation of Flame Measurements
       with the Scanning Spectrometer (Bound
       Separately)

    D. Detailed Description of Experimentation

LIST OF TABLES

iii

LIST OF FIGURES

I. ABSTRACT

This report summarizes and describes an extensive spectroradiometric study of the radiation produced in the 0.43 micron - 1.17 micron region by flames resulting from the combustion of magnesium with the alkali and alkaline earth nitrates and with sodium perchlorate at an ambient air pressure of 630 torr. Both fuel rich and stoichiometric compositions were studied.

Additional studies were made of the influence of the ambient air pressure on the combustion of a 57% Mg, 38% $NaNO_3$, 5% Laminac composition at ambient air pressures ranging from 760 torr to 1 torr to determine quantitatively the decline in output.

It has been shown that 1) burning rate, radiance and luminance decrease exponentially as the ambient pressure is decreased, and quantitative expressions are derived for these changes, 2) the ratio of visible to total radiation increases as the pressure decreases, 3) sodium perchlorate compositions radiate considerably more in the region 0.8-1.17 micron than sodium nitrate compositions, 4) a central zone of the flame radiates more energy from stoichiometric compositions than from fuel rich compositions, 5) flame temperatures computed from the spectra agree with the theoretical predictions within experimental error, 6) reasonable emissivity value in the region of the D lines can be estimated, 7) the energy radiated in a particular spectral region can be maximized by a proper choice of the oxidizer cation.

II. INTRODUCTION

Beginning in 1964 a series of studies (1-5) were initiated to investigate in considerable detail the processes occurring in the flames produced during the combustion of solid pyrotechnic fuel-oxidizer compositions. As information was gained, the methods of investigation and the analysis of the data become more quantitative and the subjects more specific. The present report is believed to represent a culmination of the first phase of these studies and should be of help to all concerned with the development of pyrotechnic systems.

This study was undertaken to determine quantitatively how the energy radiated between 0.43 micron and 1.17 micron from certain pyrotechnic flames is distributed under normal and reduced ambient air pressure. The compositions studied were those employing materials which have been useful in the manufacture of pyrotechnics and which are readily available on the commercial market. The spectral region studied includes the visible and the near infrared, in order to provide data on the radiation from the alkali elements' resonance lines. It happens that this region also includes the range of wavelengths to which several types of electronic sensors or aids to vision respond strongly. The data are therefore useful not only for the design of illuminating and signalling flares for visual use, but also for those which provide near-infrared illumination. Because the spectroradiometric data are quantitative rather than relative, it is possible to compare the results obtained from stoichiometric compositions with those from fuel-rich compositions and conclude which of these is to be preferred. Also, the reason for the superiority of sodium as a component of visual illuminating

flares has been confirmed by putting its performance in a quantitative relation to other materials, such as barium, under strictly comparable conditions of measurement.

Because of the ease with which data can be treated once they have been introduced into a computer, it has been possible to provide a number of results that will be of value to the pyrotechnist. These include colorimetric data and tables enabling the calculation of the radiation between any two wavelengths in the tabulated range.

Caution is essential to avoid being misled when the data on candle seconds per gram, intensity, etc., in this report are compared with values reported in the pyrotechnic literature. Generally speaking, these latter data are obtained under conditions that produce values which represent radiation from entire flame, and in the case of sodium-based illuminant compositions burning at sea level are of the order of 15,000-50,000 candlepower seconds per gram. The values of roughly 400 cd-secs/gm quoted in the present report are approximately 1% of those which some readers may expect, simply because of the small area of the flame from which they were obtained. Similar considerations apply to the other radiation measurements, which are described in detail in Appendix D. The compositions of the flares are listed in Table D-1, Appendix D.

3

III. DISCUSSION

The body of data which is presented in this report is the result of an effort to further the work being done at various laboratories - NAD-Crane, Picatinny Arsenal, Eglin AFB - to place the design of pyrotechnic illuminants on a sound scientific and engineering basis. Certain general trends have been made apparent which can be utilized to improve the design of illuminating compositions and much new basic data is presented which will provide a greater insight into the mechanisms which control the product of light and color by pyrotechnic flames.

A useful summary table of related information appears on page 6-46 of AMCP-706-185, Engineering Design Handbook, Military Pyrotechnics Series, Part One, April 1967.

The two major variables chosen for study were 1) the influence of the ambient pressure in which the combustion occurs, and 2) the cation of the oxidizer. In addition, the nitrates and perchlorates of sodium were both included as oxidizers to provide a comparison between two materials which experience has shown to be of great practical value in the formulation of pyrotechnic compositions.

The experimental conditions are given in detail in Appendix D. The various compositions were pressed into 33 mm i.d. fiber cases and burned in a steel chamber provided with ports through which the flames could be studied with a scanning spectrometer and a 1.5 meter grating spectrograph under selected ambient pressures.

A. Pressure Study

From the data taken on flares containing 57% Mg, 38% $NaNO_3$, 5% laminac

4

shown in Table 1, "Summary of Results from the Pressure Study," the
marked decrease in radiance which occurs as the ambient pressure is decreased
is readily apparent. This quantitative information on the pressure decre-
ment is important because of its application in the design of flares for
high altitude applications. It is also important because it provides a
part of the data needed to analyze the mechanisms of the flame reactions;
this analysis is needed if a successful mathematical model is to be created.
In the long run, the latter application will probably be the more important
one.

When the data on duration vs. pressure are plotted (see Figure 1) it
is found that the burning rate can be described by an equation of the form

$$t = KP^n \qquad p \geqq 5 \text{ torr}$$

in which t = burning duration, seconds; P = ambient pressure, torr and K
is a constant. For these particular flares, $n = -1/3$ and $K = 63$; the value
of n is believed to be typical for a wide range of compositions and sizes,
while the value of K probably typifies a specific composition. At values
of p less than 5 torr, combustion is uncertain and the divergence from the
value predicted by this equation is not surprising. A careful study of
combustion at pressures below 5 torr should be undertaken to determine
whether the same law applies or a new mechanism is occurring. At pressures
from 5 torr to 760 torr, the burning time is inversely proportional to the
cube root of the pressure. Now consider the data concerning the radiant
intensity and the power - which is a function of the ambient pressure -
furnished by the combustion of the flare composition, which are described
by the following equations for the flares studied:

$$I = K_1 P^n \text{ and } E = K_2 P^q$$

Figure 1. Pressure vs Duration or Output
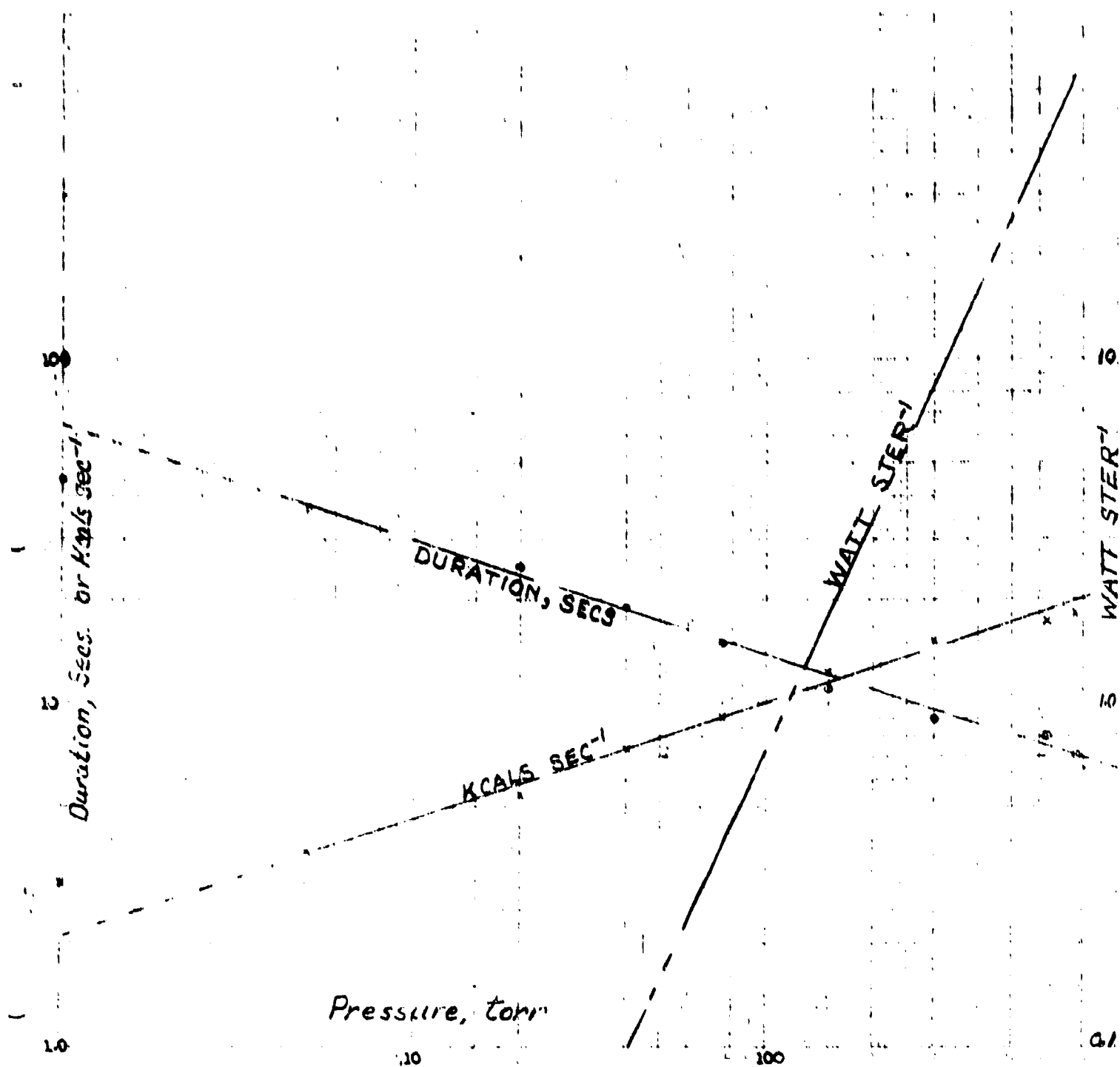
TABLE 1

SUMMARY OF RESULTS FROM THE PRESSURE STUDY

CATION ELEMENT	AMBIENT PRESSURE, TORR	ΔH KCAL GM^{-1}	BURN TIME SECS	RATE GMS SEC^{-1}	RATE KCALS SEC^{-1}	INT., WATTS STER^{-1}	INT., LUMENS STER^{-1}	CANDLE SECS. GM^{-1}
Na	760	2.02	7	9.7	18.2	65.8	5300	545
Na	630	2.02	8	8.5	17.2	21.6	3630	427
Na	300	2.02	9	7.6	15.3	15.1	2615	345
Na	150	2.02	11	6.2	12.3	1.4	243	39.3
Na	75	2.02	15	4.5	9.1	0.38	52	13.7
Na	40	2.02	19	3.6	7.4	0.09	26	7.3
Na	20	2.02	25	2.7	5.4	0.05	12	4.4
Na	5	2.02	37	1.8	3.7	0.0077	2.0	1.1
Na	1	2.02	45	1.5	3.0	0.0019	0.26	0.17

7

In which E = kilocalories sec^{-1}, I = watts $ster^{-1}$ and P = torr. From the data obtained in the present case, $K_1 = 4.0 \times 10^{-5}$, n = 2.16, K_2 = 2.0 and q = 0.35.

Comparing these equations, it is of interest to note the exponential decrease in the rate at which power is generated by the burning composition. From this observation the radiant output of the flame also would be expected to change exponentially as a function of the pressure. That is to say, the decrease in burning rate of the composition with decreased ambient pressure follows an exponential law and a corresponding reduction in radiated power would be anticipated. However, the reduction in radiant intensity is considerably greater than the reduction in the rate of energy release, as can be seen from the exponents in these relations. It is hypothesized that inasmuch as a finite area of flame was measured, it may be that the radiance has been further decreased by the expansion of the flame at lower pressures, in addition to the intensity change that is anticipated from the decrease in burning rate. This implies a reduction in the number of radiators per unit volume (or area) with, perhaps, a reduction in the percentage of possible radiators that have been excited. The reduction in the number of excited atoms would be expected from the decrease in the rate at which atomic species are created as the burning rate is decreased; a lowered flame temperature which may result from the lower rate of energy release would create fewer excited atoms and/or molecules.
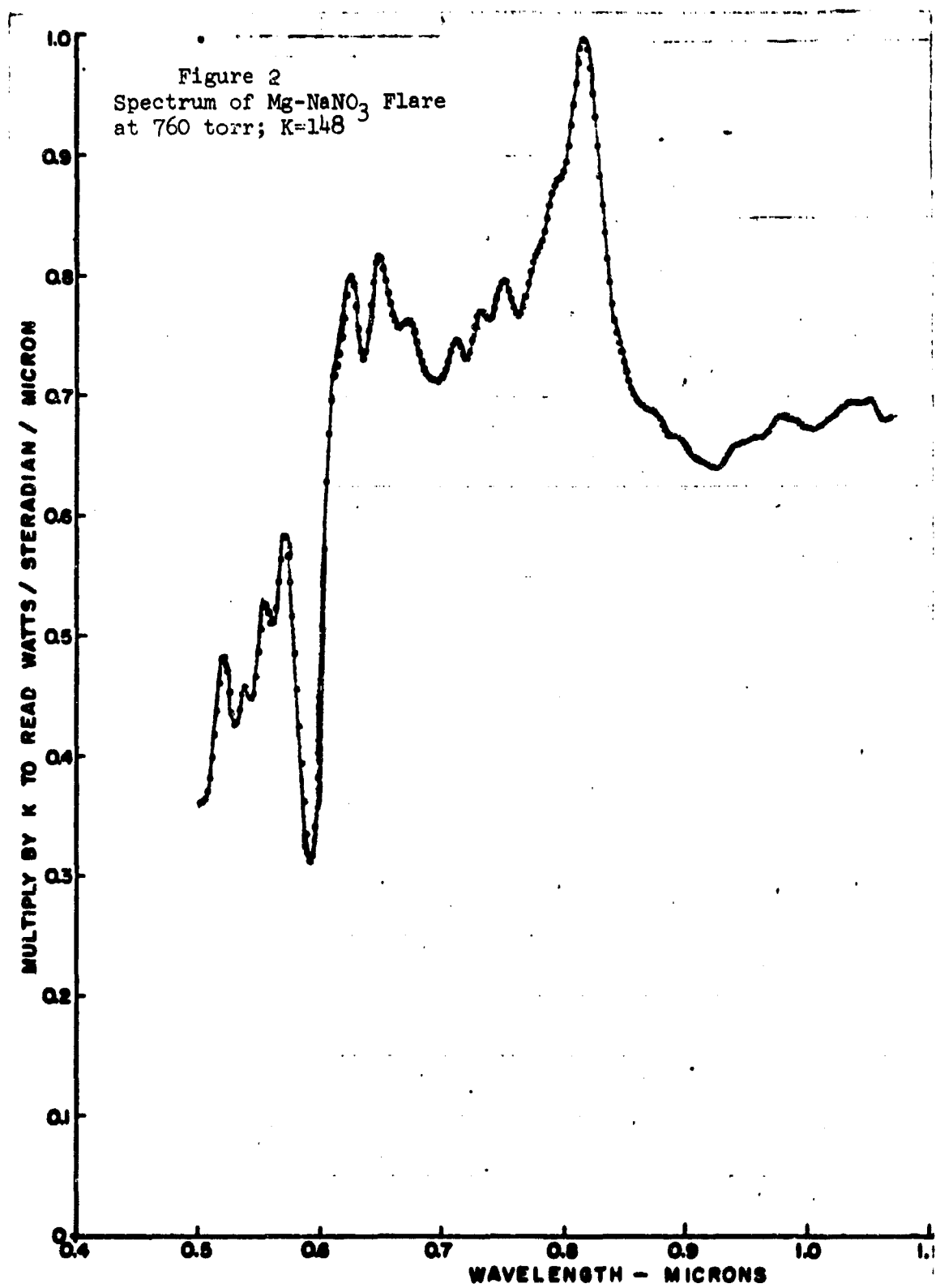
The reduction in the effectiveness of flares as illuminants when combustion occurs at the reduced pressures of high altitutdes has been known for some time and various compositions have been described as useful in minimizing the effect. From the present quantitative results it appears that empirical changes in the composition do not attack the source of the

8

problem effectively. Studies should be directed toward the discovery of effective means of maintaining the flame temperature and the concentration of the emitting species.

As a final comment, it is interesting to note in Table 1 from columns 7 and 8 that the ratio of visible radiation to the total radiation measured increases at low pressures. This is quite evident in Figure 2 through 6. In these spectra, it is evident that at higher pressures a large amount of power is radiated in the region beyond 0.65 micron, which is wasted so far as visual effectiveness is concerned. As the pressure is reduced the amount of power radiated in this longer wavelength region relative to that produced between 0.45-0.65 micron (due primarily to excited Na atoms) is greatly diminished. The desirability of research aimed at utilizing this observation by finding methods of increasing the concentration of useful radiators in the flame and maintaining high flame temperatures independently of the ambient pressure condition is apparent.

The investigation of pressure-related phenomena was stopped at this level in order to round out the desired coverage of the present study by a series of measurements on composition-related effects. This does not mean that the pressure studies are considered as completed. For example, an Arrhenius type of plot of the burning rate in kilocalories per second vs. reciprocal pressure can be constructed from the data in the summary table, which shows a change in rate at approximately 100 torr. By extending the range of these measurements and simultaneously determining the number of moles of nitrogen and sodium vapor, data concerning the Mg-$NaNO_3$ rate-controlling reaction can be obtained. These data also will be needed in the construction

9

Figure 2
Spectrum of Mg-NaNO$_3$ Flare
at 760 torr; K=148

MULTIPLY BY K TO READ WATTS/ STERADIAN / MICRON

WAVELENGTH — MICRONS

Figure 3
Spectrum of Mg-NaNO$_3$ Flare
at 300 torr; K=67.4^3

11

Figure 4
Spectrum of Mg-NaNO$_3$ Flare
at 150 torr; K=11.2

Figure 5
Spectrum of Mg-NaNO$_3$ Flare
at 75 torr; K=2.61

13

Figure 6
Spectrum of Mg-NaNO$_3$ Flare
at 1.0 torr; K=0.016
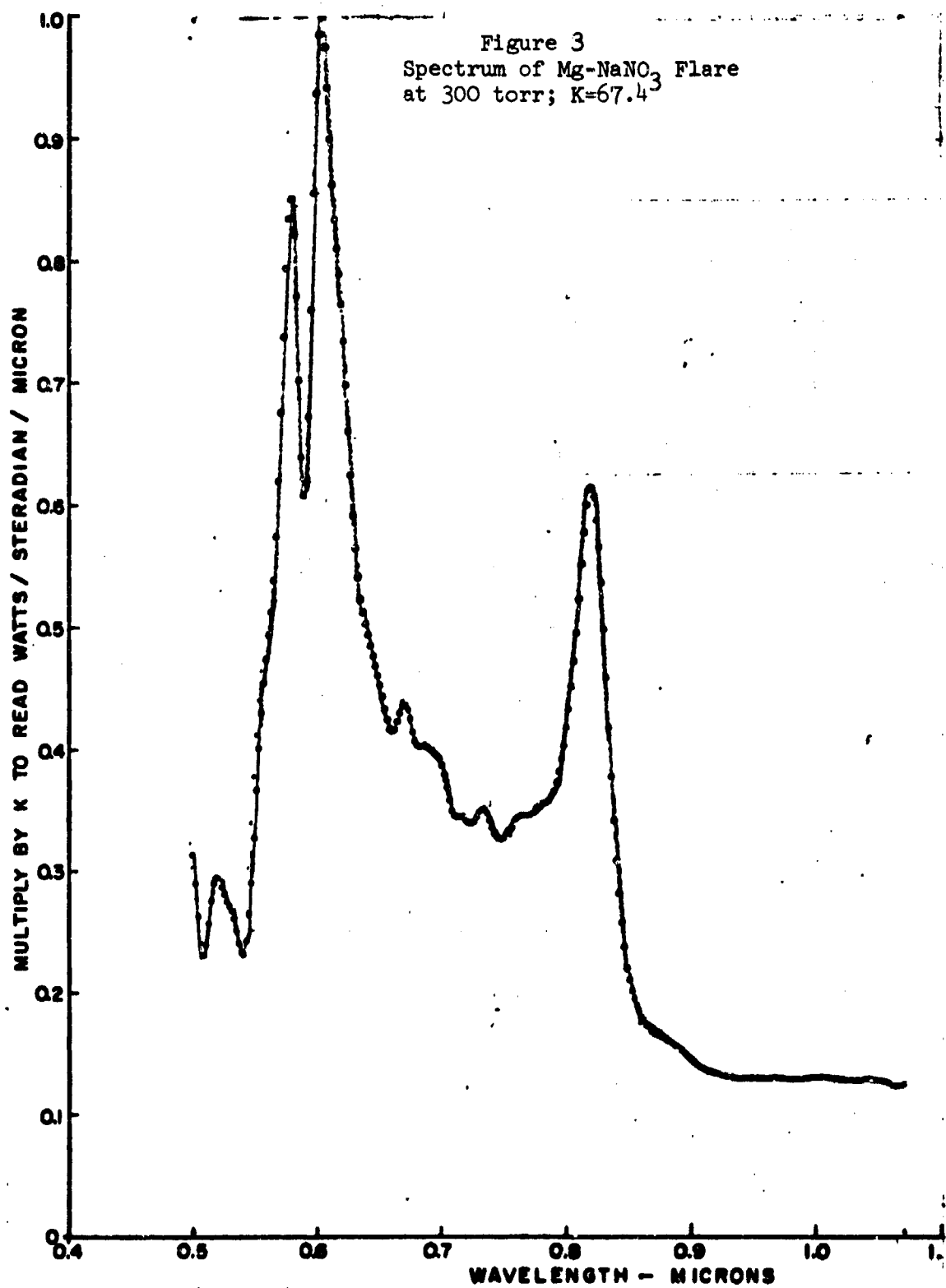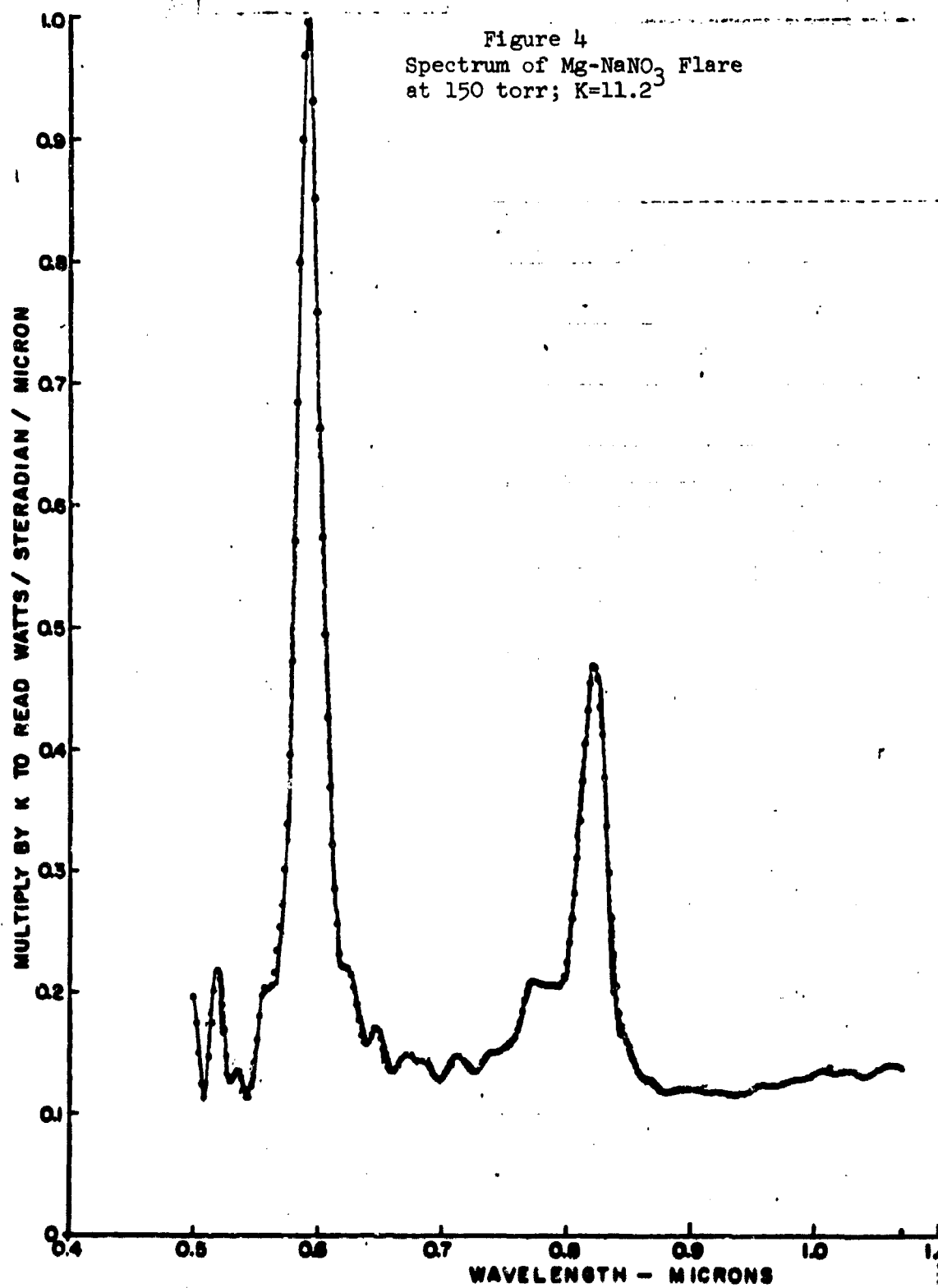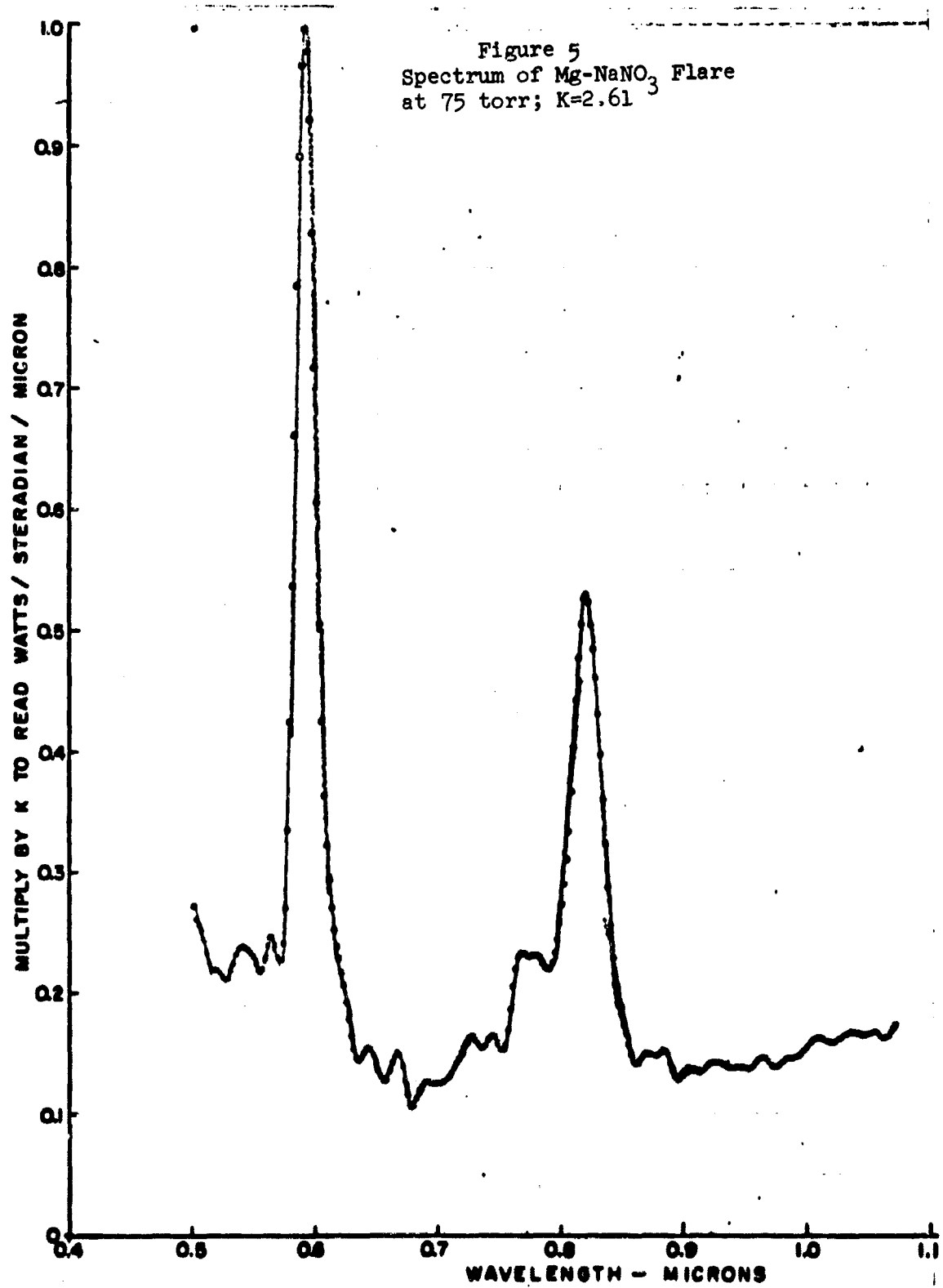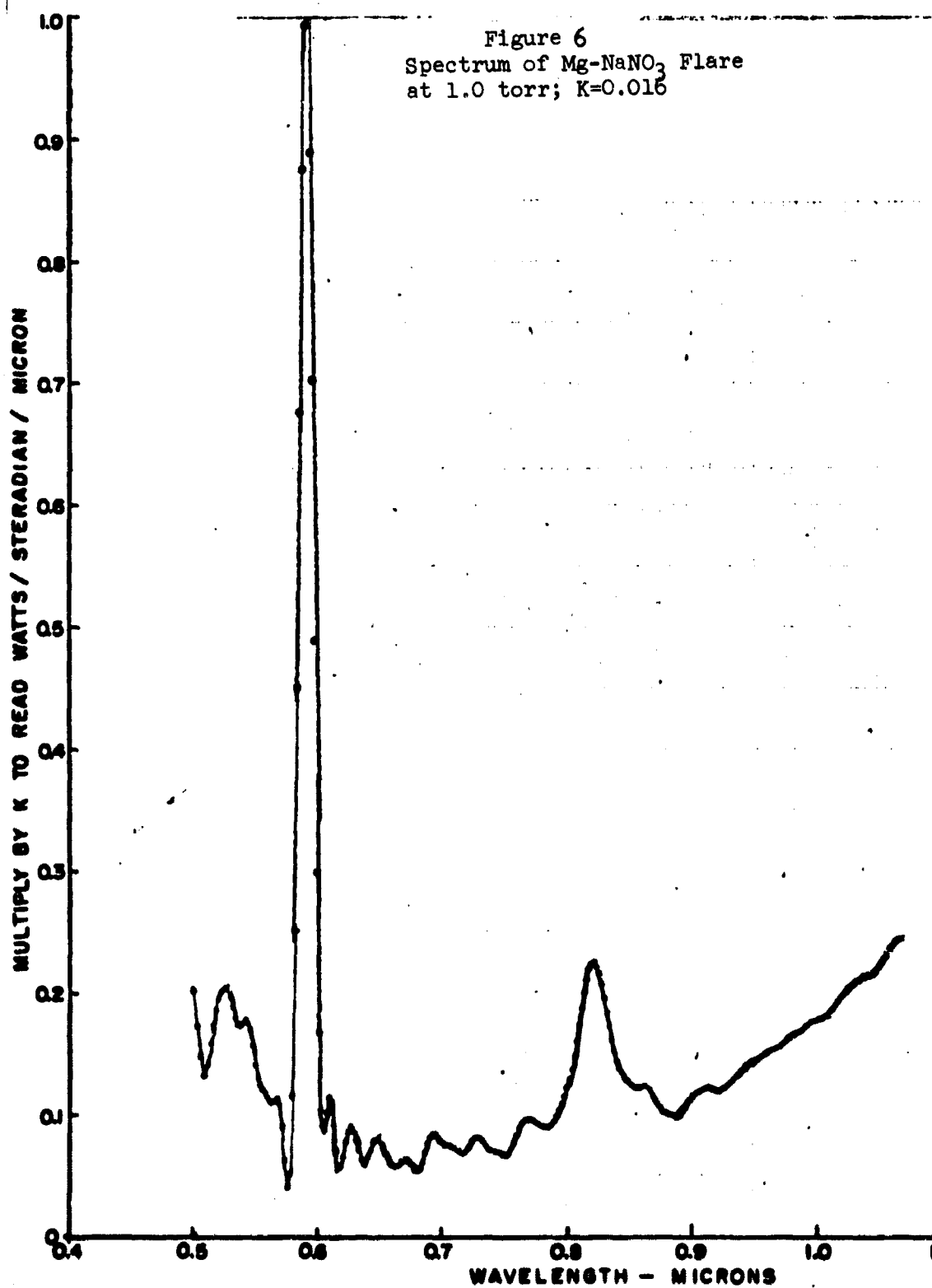
of a rational model which can predict flare behavior and design parameters, for whatever compositions are of interest. It can only be obtained by experimental work of the general nature performed in the present study.

B. Composition Study

The next phase of the study was an investigation of the power distribution of the radiation in the 0.43-1.17 micron spectral range that is produced by the alkali and alkaline-earth cations when the corresponding nitrates are employed as oxidizers.

REMOVED DURING REVIEW BY NAD CRANE

From the quantitative measurements that were made of the radiation produced by the flames of stoichiometric compositions, and compositions containing a fixed ratio of oxygen to fuel, it is possible to show certain general trends that should be considered in the design of flares. The data obtained in this phase have been summarized for discussion in Table 2 and Figures 7 and 8.

Comparison of the energy radiated per gram from the central region of the flame from these compositions shows very clearly in Figure 9 that the

TABLE 2

SUMMARY OF SPECTROGRAPHIC AND RELATED RESULTS
FROM 0.43–1.17 MICRONS, COMPOSITION STUDY

	ELE-MENT	FLARE CODE	KCAL GM⁻¹	BURN TIME SECS	RATE GMS SEC⁻¹	RATE KCALS SEC⁻¹	WATT SEC GM⁻¹	INT., WATTS STER⁻¹	INT., LUMENS STER⁻¹	CANDLE SECS. GM⁻¹	APPARENT LUMENS WATT⁻¹	DOMINANT WAVE LENGTH MICRONS	EXCIT. PURITY %
1	Li	B-1	2.20	17.1	2.92	6.43	71.1	16.5	1258	430	0.59	9.589	59.3
2	Na	B-2	2.02	15.9	3.16	6.37	67.5	17.0	2076	658	0.98	0.586	70.5
3	K	B-3	1.80	18.9	2.65	4.76	145.7	30.7	761	288	0.48	0.589	53.6
4	Rb	B-4	1.44	21.5	2.33	3.36	139.0	25.8	683	293	0.61	0.585	41.0
5	Cs	B-5	1.18	25.0	2.00	2.37	159.6	25.5	618	309	0.78	0.584	53.3
6	Mixed	B-17	2.37	22.7	2.20	5.22	142.6	25.0	1009	458	0.58	0.589	71.0
7	Na ClO4	B-19	2.65	22.1	2.27	6.01	157.7	28.5	2517	1110	1.3	0.585	63.4
8	Li	B-9	3.19	11.3	4.44	14.2	24.6	9.7	531	119	0.11	0.593	64.4
9	Na	B-10	2.93	14.1	3.56	10.4	38.3	10.8	1651	464	0.47	0.587	81.9
10	K	B-11	2.71	16.0	3.13	8.47	87.7	21.8	473	151	0.17	0.590	57.4
11	Rb	B-12	2.29	17.4	2.87	6.58	76.1	17.4	329	114	0.15	0.589	56.3
12	Cs	B-13	1.93	18.6	2.70	5.2	107.1	23.0	486	180	0.28	0.583	55.5
13	Mixed	B-18	2.62	18.3	2.73	7.16	73.1	15.9	536	196	0.22	0.589	77.6
14	Na ClO4	B-20	3.30	18.4	2.72	8.97	153.5	33.2	2486	915	0.83	0.585	65.6

TABEL 2 (Cont'd.)

SUMMARY OF SPECTROGRAPHIC AND RELATED RESULTS
FROM 0.43-1.17 MICRONS, COMPOSITION STUDY

	ELE-MENT	FLARE CODE	KCAL GM^{-1}	BURN TIME SECS	RATE GMS SEC^{-1}	RATE KCALS SEC^{-1}	WATT SEC GM^{-1}	INT., WATTS STER^{-1}	INT., LUMENS STER^{-1}	CANDLE SECS. GM^{-1}	APPARENT LUMENS WATT^{-1}	DOMINANT WAVE LENGTH MICRONS	EXCIT. PURITY %
1	Ca	B-6	2.26	37.8	1.33	2.99	60.4	6.4	695	525	0.70	0.592	76.7
2	Sr	B-7	1.88	27.6	1.81	3.41	140.7	20.3	894	493	0.79	0.594	66.6
3	Ba	B-8	1.61	19.6	2.55	4.11	188.4	38.2	1626	637	1.19	0.583	59.3
4	Ca	B-14	3.62	31.0	1.62	5.85	34.5	4.43	452	280	0.23	0.593	83.4
5	Sr	B-15	2.93	19.4	2.58	7.55	50.3	10.3	284	110	0.11	0.601	84.3
6	Ba	B-16	2.67	14.2	3.53	9.44	47.0	38.2	358	101	0.11	0.582	62.5

Figure 7.

Spectral Radiant Intensities of the Alkali Metal
Compositions Individually and Mixed
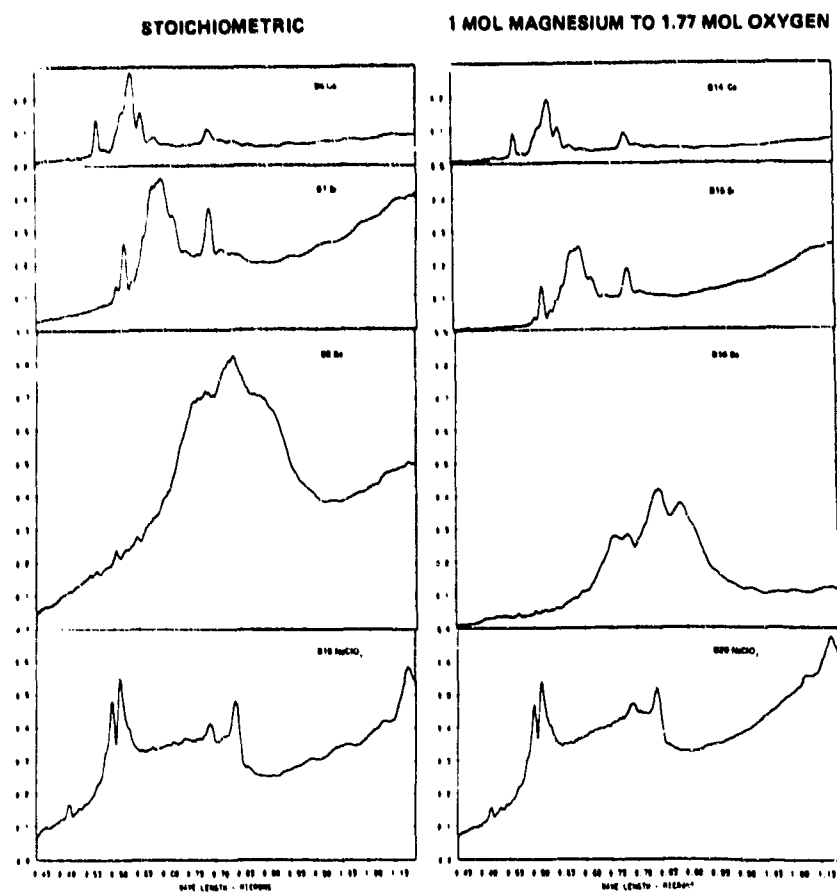
Figure 8.

Spectral Radiant Intensities of the Alkaline Earth Metals and
Sodium Perchlorate Compositions

200   ⊙ Alkali Nitrate, Stoichiometric
       × Alkali Nitrate, 1 mol Mg to 1.77 md O$_2$
       △ Alkaline Earth Nitrate, Stoichiometric
       ▣ Alkaline Earth Nitrate, 1 mol Mg to 1.77 mol O$_2$

ENERGY, WATT SECS/GRAM

150

100

50
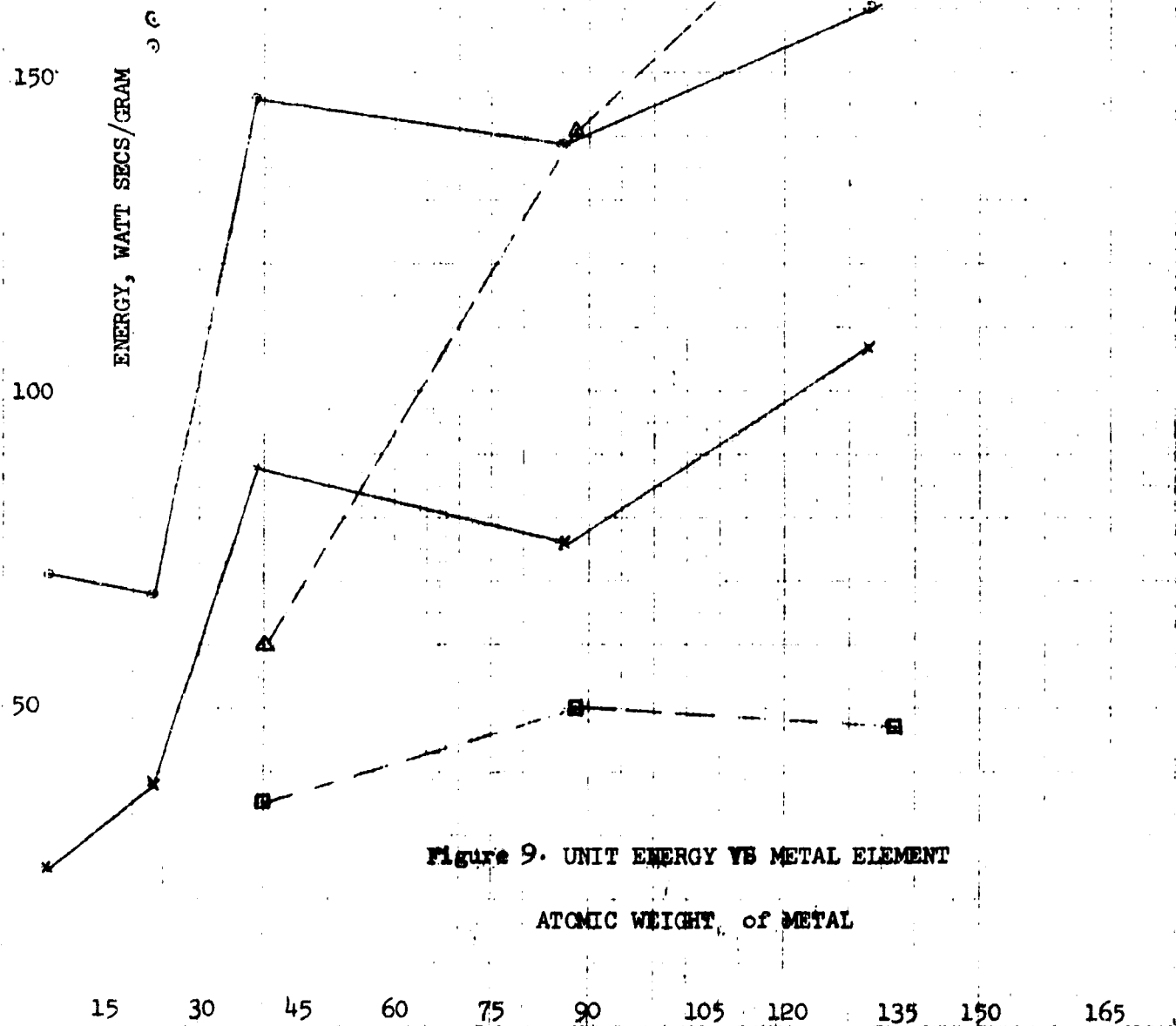
Figure 9. UNIT ENERGY VB METAL ELEMENT

ATOMIC WEIGHT of METAL

15   30   45   60   75   90   105   120   135   150   165

20

stoichiometric composition is more efficient in all cases. In view of the greater radiance produced by fuel-rich compositions that is normally observed from magnesium-sodium nitrate illuminating composition, this result was unexpected. However, candlepower measurements made in the ordinary way are taken of the radiation produced by the entire flame area, whereas in the present studies the radiation studied came from a small region (See Appendix D) of the flame. It is concluded that *the difference in the relative efficiency is a consequence of the difference in the radiation produced by the small, central area of the flame and that from the entire flame.* In view of the rather large change that occurs between total flame and local flame radiance, it would be worthwhile to study these flames in a mapping process to examine this phenomenon in greater detail.

Various hypotheses can be advanced to account for this difference, but at the current state of knowledge of these processes they would probably represent only interesting speculations.

As the atomic weight of the alkali cation increases, the amount of energy radiated per gram also increases, as is evident from Figure 11, from which it may be concluded that the stoichiometric composition which contains the oxidant of highest molecular weight will produce the greatest amount of radiant energy per gram of mix burned. The ratios of the radiated energies from the stoichiometric mixes to those from mixes containing a constant ratio of 1.77 mol oxygen per mol of magnesium range from 2.9 to 1.7 as the atomix weight of the oxidizer cation increases as may be seen in Figure 10.

The MK 24 flare candle uses essentially the same composition as the 38.0% $NaNO_3$, 57% Mg, 5% binder mix used in the present tests. An increase
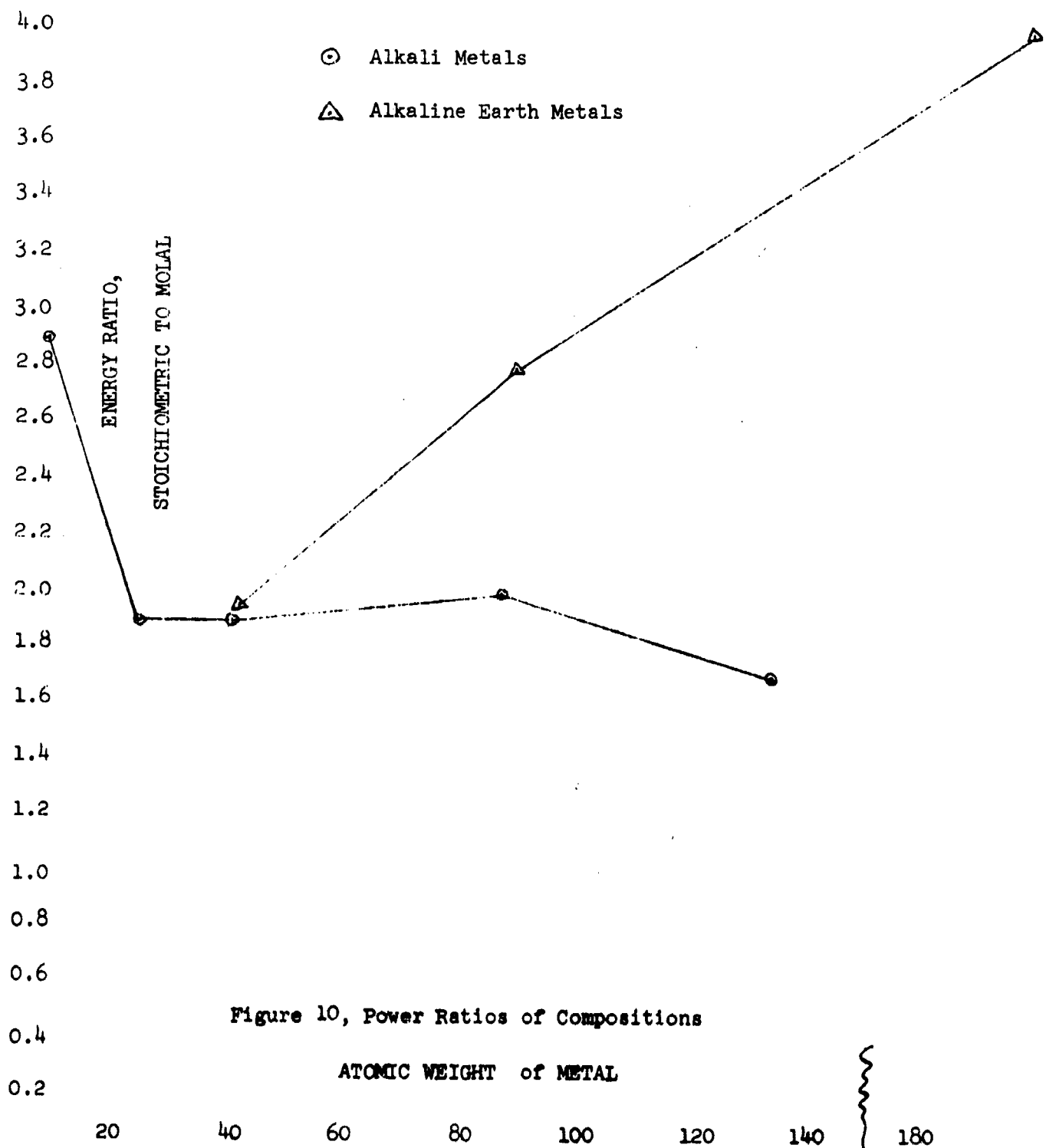
Figure 10, Power Ratios of Compositions

⊙ Alkali Metals

△ Alkaline Earth Metals

ENERGY RATIO, STOICHIOMETRIC TO MOLAL

ATOMIC WEIGHT of METAL

in radiated energy per gram of 1.7 times is obtained from the stoichiometric formula of 51.5% $NaNO_3$, 43.8% Mg, 5% binder; *if this central radiance ratio can be produced throughout the flame,* a considerable performance gain would result.

Comments analogous to the above can be made even more positively with regard to the alkaline earth nitrate compositions. Similar plots of the results produced by the combustion of stoichiometric and constant mol ratio mixes of calcium, strontium and barium are included in Figures 7-11. It is apparent that with these materials the stoichiometric compositions radiate more energy per gram than do the fuel rich compositions and that this trend becomes more pronounced as the atomic weight of the nitrate increases. The effect is more pronounced for the alkaline earth nitrate mixes than for the alkali nitrate mixes.

If the power, rather than the energy per gram, is of major interest to a particular designer it may be seen from comparisons of the watts/steradian values in Figure 11 that a condition exists similar to that found with the energy values.

However, when the luminous intensity values are compared, the striking superiority of flares containing sodium becomes immediately apparent. Further, perchlorate mixtures which contain an equal number of sodium atoms are superior to those based on the nitrate by approximately 20% as is evident in Table 2 and Figure 12.

Efficiency in the production of light may be considered as the consequence of the coordination of two factors. One is the efficient production of radiant power, the second is the concentration of that power in a desired region to the greatest possible extent. A flare containing sodium almost automatically produces power in the visible region as a consequence of the

23

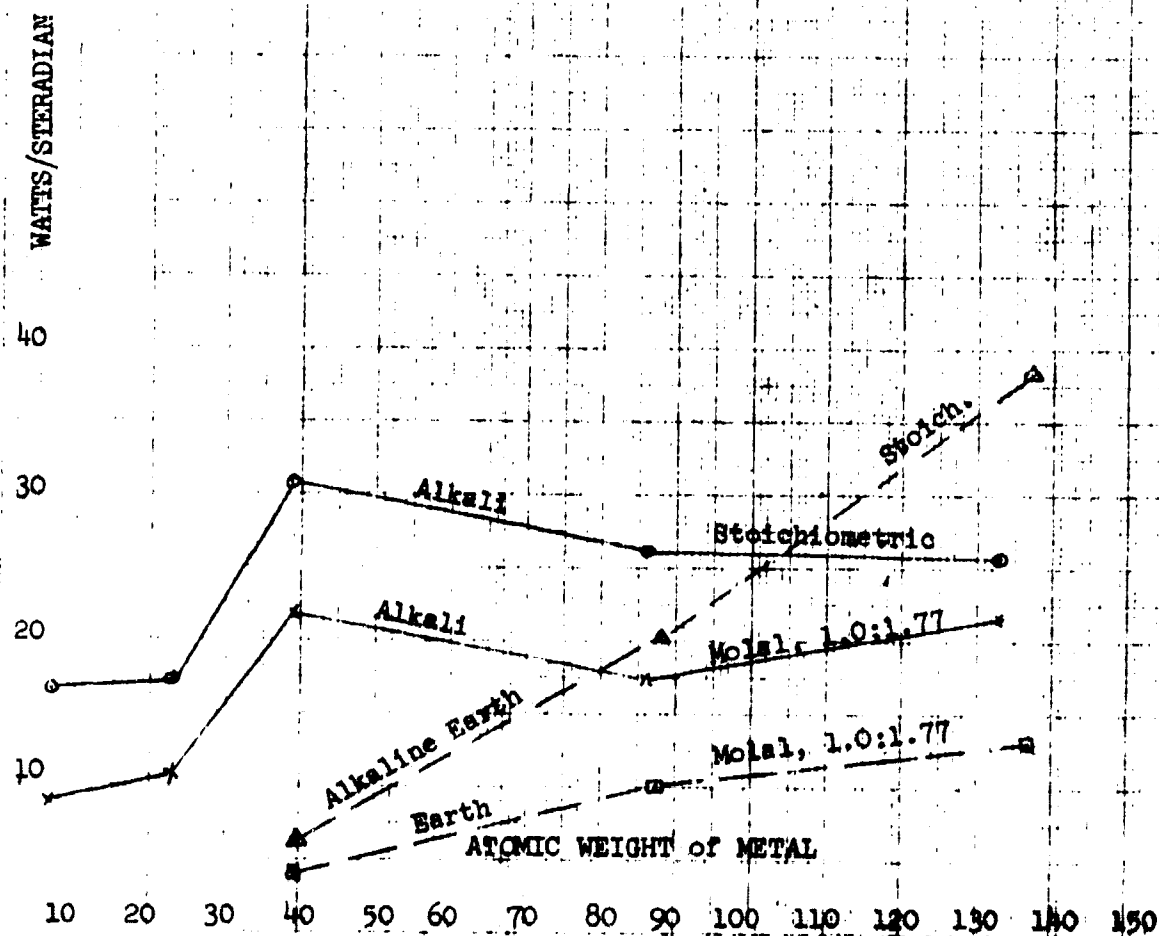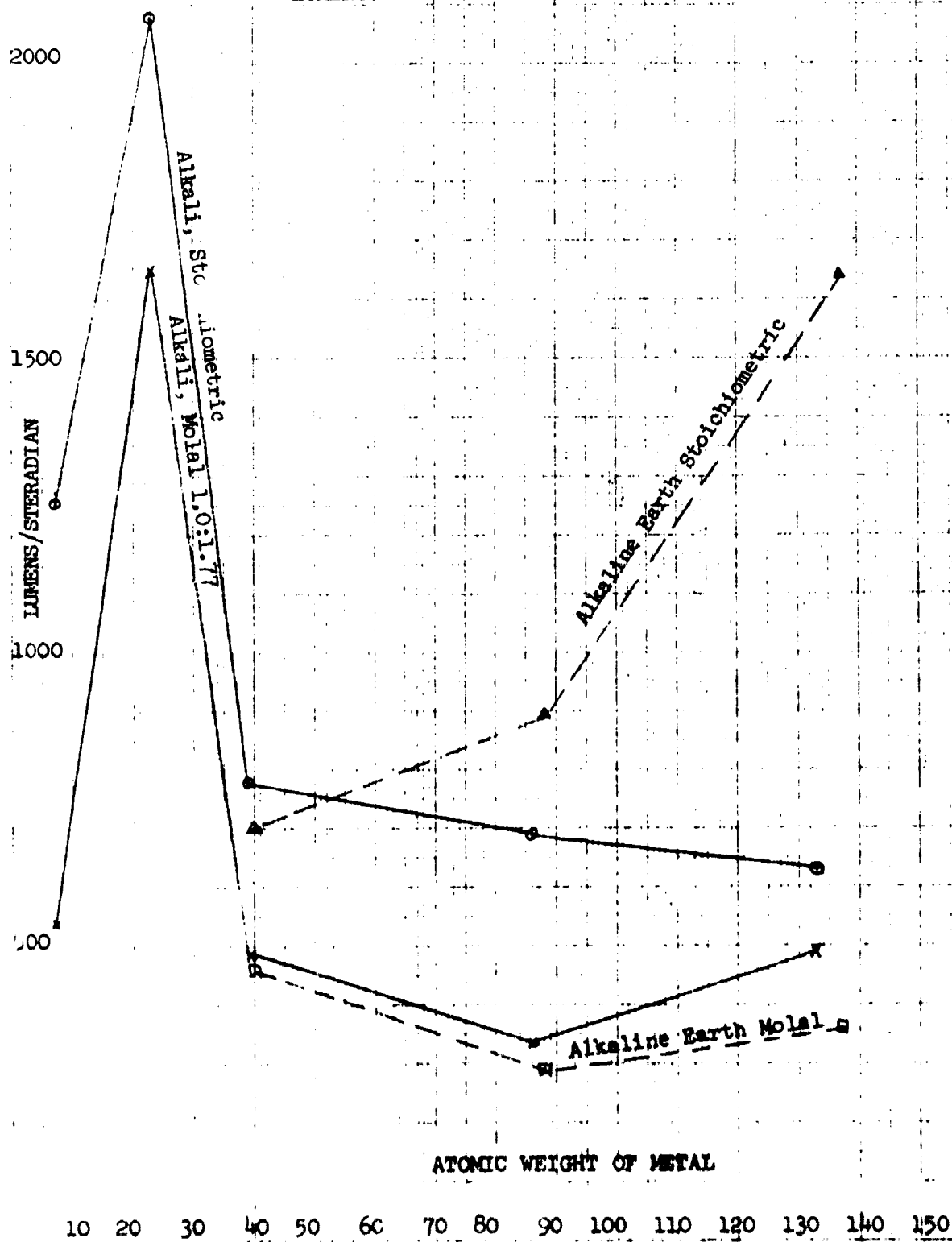Figure 11

RADIANT INTENSITY VS METAL ELEMENT

Figure 12

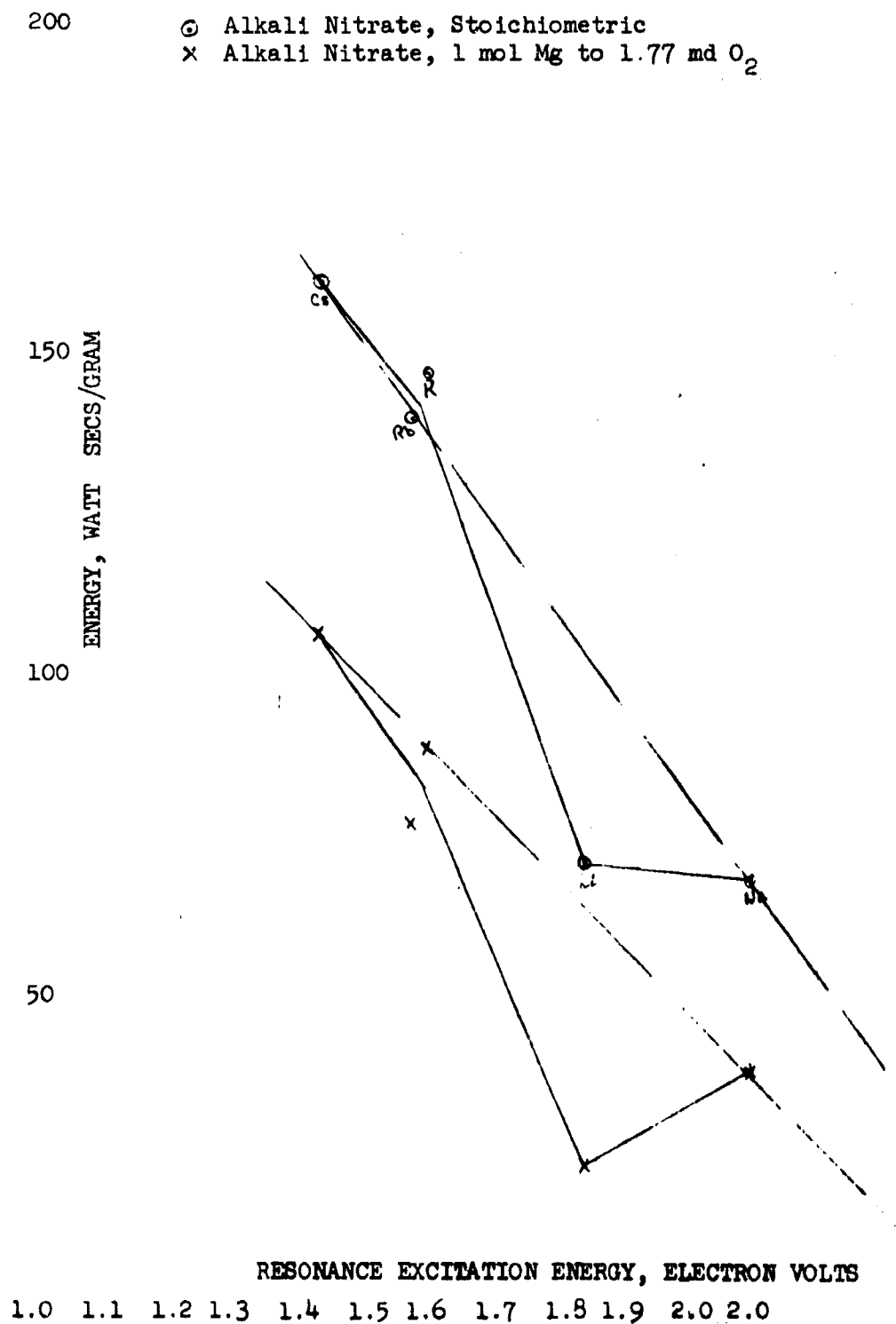LUMINOUS INTENSITY VS METAL ELEMENT

25

atomic structure of this alkali. The resonance radiation of sodium lies in the region to which the eye is most sensitive, while resonance radiation from the other alkali metals lies in the near infrared. Because the resonance radiation from any one atomic species requires the least energy for its excitation it tends to be the dominant spectral feature. The excitation energy required by the sodium resonance lines is roughly 14% greater than is needed by lithium and 50% greater than needed by cesium. The flame temperature determines the excitation energy available and, while other factors also affect the radiation intensity, would produce at a certain low temperature only cesium radiation, followed by rubidium, potassium, lithium and sodium as the temperature is increased. Then, at a given temperature less radiation from sodium than from, say, cesium, might be expected. That is believed to be the fundamental explanation for the shape of the curves in Figure 9 and Figure 13 from which it is seen that essentially this relation is followed by the alkali metals. As a result, the sodium flare should exhibit a greater loss of radiance with decreasing flame temperature than, say, cesium. Since it appears that a drop in flame temperature occurs as the ambient pressure is lowered, use of cesium in non-visual tracking flares would minimize the reduction in radiance at high altitudes.

The radiation from the alkali metals is basically atomic, modified by high temperature and atom concentrations to produce a considerable amount of continuum radiation. Even so, the predominant feature of these spectra is the line structure which is evident in the spectrograms in Appendix B. The alkaline earths, however, produce spectra which exhibit several lines, but are really characterized by band structure from excited molecules such

26

Figure 13

RADIANT ENERGY VS RESONANCE EXCITATION ENERGY
of ALKALIES

200   ⊙   Alkali Nitrate, Stoichiometric
          ✕   Alkali Nitrate, 1 mol Mg to 1.77 md O_2

RESONANCE EXCITATION ENERGY, ELECTRON VOLTS

1.0   1.1   1.2 1.3   1.4   1.5 1.6   1.7   1.8 1.9   2.0 2.0

27

RO and ROH. These bands are evident in the spectrograms of the alkaline
earth compositions shown in Appendix B. The resolution of the spectrograms
is quite good, whereas in the spectral intensity plots that are contained
in Appendix A it is impossible to see the fine structural details. Thus,
the major emitters are easily identified from the grating spectra while
the power radiated at various wavelengths can be seen directly from the
intensity plots. The alkali nitrates produce intensity plots which are
characterized by a spike-like shape, riding on a general background level
of radiation which is typically from 5% to 20% of the spike amplitude.
The alkaline earths produce a greater level of background in proportion to
the spikes. A progressive change is apparent in passing from calcium,
which still has a predominant spike structure, to barium, which exhibits
no spikes but a broad hump in the near infrared.

Examination of Figure 12 reveals that barium is the nearest competitor
to sodium in luminous intensity, when employed in a stoichiometric formula-
tion. Special reasons might dictate the use of an oxidizer that does not
contain sodium, in which event the barium compositions should be considered.

The reasons for the general inferiority of the alkaline earths as pyro-
technic illuminants are apparent from the radiant intensity plots, where
the general predominance of band structure results in the production of
radiation which is distributed throughout the spectrum instead of being
concentrated in a few locations which happen to be visually quite effective
as is true of the radiation from sodium flames. The addition

28

of halogens, such as chlorine or fluorine, to barium compositions causes the production of intense bands in the green region due to BaCl or BaF molecules. These compositions are useful as green signals although degradation of the color purity by the bands outside the green region is difficult to overcome. However, neither calcium, strontium or barium can compete with sodium as an illuminant for the reasons given above.

In conjunction with the above comments on the use of halogens to shift the radiation pattern into a preferred region of the spectrum notice should be taken of the effect of chlorine in sodium compositions. Compare the radiant intensity plots in Appendix A for B-2 and B-10 flares with those for B-19 and B-20 flares. At approximately 0.55 microns a shoulder or jog is apparent in the B-2 and B-10 spectral plots which does not appear in the B-19 or B-20 spectra. The same phenomena is observable on the grating spectrograms in Appendix B. At the same time, note the great increase in the energy radiated beyond 0.78 micron by the perchlorate compositions as compared to the nitrates. An explanation for these changes may be that a different flame species is created in the presence of chlorine which radiates in the near infrared. The phenomenon should be studied further because it may provide important clues to the reactions which occur at the temperature of the flame, currently not well understood.

C. Flame Temperatures

The experimental values of absolute radiant intensity can be used to calculate a temperature on the assumption that the flame is radiating as a gray, or black, body would. That is, the emissivity of the flame is assumed either to be independent of temperature and wavelength, or to be

known. If the emissivity is truly independent of temperature and wavelength then by the use of a modified equation it can be eliminated from the calculation.

The flame is not in general a black or graybody radiator, but some evidence exists that it may behave at certain specific wavelengths as though it were. This condition requires that the flame, over a narrow spectral region, be of the same radiance as that which a blackbody would produce; this, it is thought, may occur in flames that are optically thick and also saturated with some selective emitter. An alkali nitrate flare flame may meet these conditions if the alkali atom concentration is high enough and the physical thickness of the flame is adequate. The alkali atom concentration can be assumed to be adequate if one accepts the view of Strong and Bundy[6] that this condition is detectable as an extreme broadening of the resonance lines. Such extreme broadening is noted at pressures of about 300 torr or more in the alkali metal flames that have been studied in this project and it has therefore been of interest to examine the temperatures calculated from the intensities measured in the region adjoining the resonance lines.

The measured values of radiance may be in error by approximately 15% (See Appendix D) and it has been deemed necessary first to estimate the temperature variation that may be expected from this uncertainty.

The brightness temperature is given by Wien's Law as

$$T = -6.25 \times 10^3 / \lambda \, (\log L + 5 \log \lambda - 4.573)$$

for an emissivity of unity. If the emissivity is not unity, the value (-4.573) must be replaced by that which corresponds to $\log (1/ec_1)$; e is

the emissivity and $c_1 = 3.741 \times 10^4$ w μ^4 cm^{-2}, L is the radiance in watts/cm^2/micron and λ is the wavelength in microns.

It may easily be calculated from this that an error of 15% in L will be reflected as an error of 30°K to 50°K in the region of 2000°K to 3000°K.

Similarly, the derived relation

$$T = (0.4343)(1.439 \times 10^4)(\lambda_2^{-1} - \lambda_1^{-1}) \div$$
$$(\log {}^L1/L_2 - 5 \log \lambda_2/\lambda_1)$$

used to compute the temperature when the emissivity is assumed to be the same at λ_1 and λ_2 may be evaluated for the change due to an error in L_1 and L_2. In the same 1000°K temperature range, an error of +15% in L_1 and -15% in L_2 - representing a "worst case" condition - would produce an error in temperature of around 2200°K.

From this it would appear desirable to compute the brightness temperatures at two wavelengths as well as the temperature from the intensity ratio at these same wavelengths. If there is more than 100°K difference between the brightness temperatures, or between them and the ratio temperature, these temperatures are probably quite meaningless because of error of measurement or failure to satisfy the assumptions. If, on the other hand, the three temperatures agree within, say, 100°K they may represent a flame temperature that can be correlated with the flame processes. Therefore, as a matter of interest, these three temperatures have been calculated as a part of the data reduction process and some are shown in Table 3. A fair agreement exists between the brightness temperatures, but they are generally around 500°K higher than the ratio temperature in the case of the sodium nitrate compositions.

TABLE 3

CALCULATED APPARENT SODIUM FLARE FLAME TEMPERATURES

Oxidant	Wavelength, microns, of Intensity Measurement				
	0.594±.005	0.577±.005	0.821±.005	0.594±.005 to 0.577±.005	0.821±.005 to (λ)
	BRIGHTNESS, °K			RATIO, °K	
NaNO$_3$	3124	3190		2765	
"	3148	3216		2869	
"	(J) 3116	3175		2520	
"	3122	3183		2698	
"	3120	3178		2599	
"	(J) 3097	3149		2356	
NaClO$_4$	3124				4886(.598)
"	3164	3203		2725	
"		3174	2484	2399	
"	(J) 3173	3206		2405	
"	3176	3220		3074	
"	3162		2541	2615	
"	3104	3148			3892(.578)
"	3162		2546	3413	
"	3110		2502	3469	
"	(J) 3169		2529	2264	

(J) From intensity values corrected for slit width.

Suppose then that saturation does occur at the 0.5890 micron region, peaking at about 0.577 micron, but does not quite exist in the region due to the 0.5896 micron line, whose intensity peaks around 0.594 microns. It would then be found that the brightness temperatures computed at the peak intensities due to these resonance lines differ and that the value obtained at 0.577 microns exceeded the 0.594 micron value. The data from sodium nitrate show that the 0.577 micron values for temperatures are indeed consistently some $60^{\circ}K$ greater than the 0.594 micron values. The difference of $60^{\circ}K$ does not at first appear to be adequate to account for the $550^{\circ}K$ difference noted between the average ratio temperature ($2635^{\circ}K$) and the average 0.577 micron brightness temperature ($3185^{\circ}K$). However, if the Wien equation is solved for the value of the emissivity needed to make these two temperatures agree, it is found that the emissivity is 0.917. This is quite a high value of emissivity compared to the theoretical maximum of 1.00. If this emissivity value is to be accepted, it should also account for the observed $60^{\circ}K$ brightness temperature difference noted before. The calculated correction amounts to $37^{\circ}K$, which is approximately two-thirds of the expected value. While the agreement is not complete, it is adequate to support this hypothesis when the measurement accuracy is recalled.

If the temperatures calculated for similar compositions by sophisticated thermochemical computer programs are examined it will be found that they range from $2600^{\circ}K$ to $3100^{\circ}K$, depending upon the exact nature of the assumptions made in the calculation.

It appears that the temperatures calculated from the data obtained in this study are realistic, agreeing fairly well with theoretically calculated

values; that there may be a difference in the emissivity at particular wavelengths in the small flares used in the study which was not suspected; and that further efforts are warranted to improve the accuracy of measurement so that better values of temperature and emissivity can be obtained for use in a flare mathematical model based on the reaction processes.

In closing this discussion it is well to note that the materials used in compounding these flares were of good commercial quality but were not especially purified. As a result, there is some residual amount of each alkali that remains in the salts of the others which is quite evident when the spectra are examined. There is undoubtedly some change in relative amplitude of the radiance produced by a given nitrate due to this lack of complete purity. On the other hand, this study is directed toward practical ends, for which reason the use of especially pure materials was not appropriate. The cost of such materials would make their use in military pyrotechnics completely uneconomical; the performance changes that would be expected, except for specialized applications, would be insignificant.

IV.   CONCLUSIONS

The marked decrease in the efficiency of illuminating compositions which has been observed at high altitudes has been substantiated and quantitative relations derived between the ambient pressure and the energy release rate, the burning rate and radiance of a typical magnesium-sodium nitrate composition. It is found that the radiance and rate both change exponentially with pressure and that a decided shift occurs in the spectral distribution of the radiation, relatively more visible radiation being emitted at lower pressures with respect to the total emitted between 0.43 micron - 1.17 microns. Some evidence was found for a change in the combustion mechanism at pressures less than 10 microns, evidenced by a change in the slope of the pressure vs rate graphs.

Both alkali and alkaline earth nitrate oxidizers produced higher radiance from stoichiometric mixes than from fuel-rich compositions, contrary to findings based on whole flame measurements. This difference must be due to a change in radiation processes which occurs in moving from the center to the outside of the flame.

With regard to the central flame zone near the candle end, the following conclusions result from these studies:

a. Stoichiometric compositions radiate more energy per gram or per second than fuel-rich compositions.

b. Stoichiometric compositions containing oxidizers with high atomic weight cations are as much as four times as effective in the production of radiant power, per gram. The same trend is observed in the fuel-rich compositions but to a lesser degree. A similar comment may be made

35

concerning radiant intensity, but again the effect is less marked.

c. Concerning luminous intensity, a similar situation exists but because of the effect of the visibility function, an enormous leverage is exerted by radiators which emit in the visible region of 0.4-0.7 micron. This is the reason for the effectiveness of sodium compositions, followed in utility by those containing barium.

d. It is found that sodium perchlorate compositions radiate much more energy than the nitrate in the region beyond 0.8 micron and should be considered when radiation is required in this region. A shoulder in the radiant intensity vs wavelength which is observed in $NaNO_3$ flames at about 0.55 micron does not occur in the $NaClO_4$ flames, indicating a change in the species present.

e. Those elements with the lowest excitation potential are the most efficient sources of radiant energy. This reinforces other considerations which require a high flame temperature for efficient radiation of useful energy.

f. Optically determined flame temperatures of the $NaNO_3$ - Mg flares have been found to agree with theoretical predictions within the experimental limits of error. Some evidence has been found that 1) these small flares are not quite optically thick and 2) that there is a small, unexpected variation in emissivity near the D-lines.
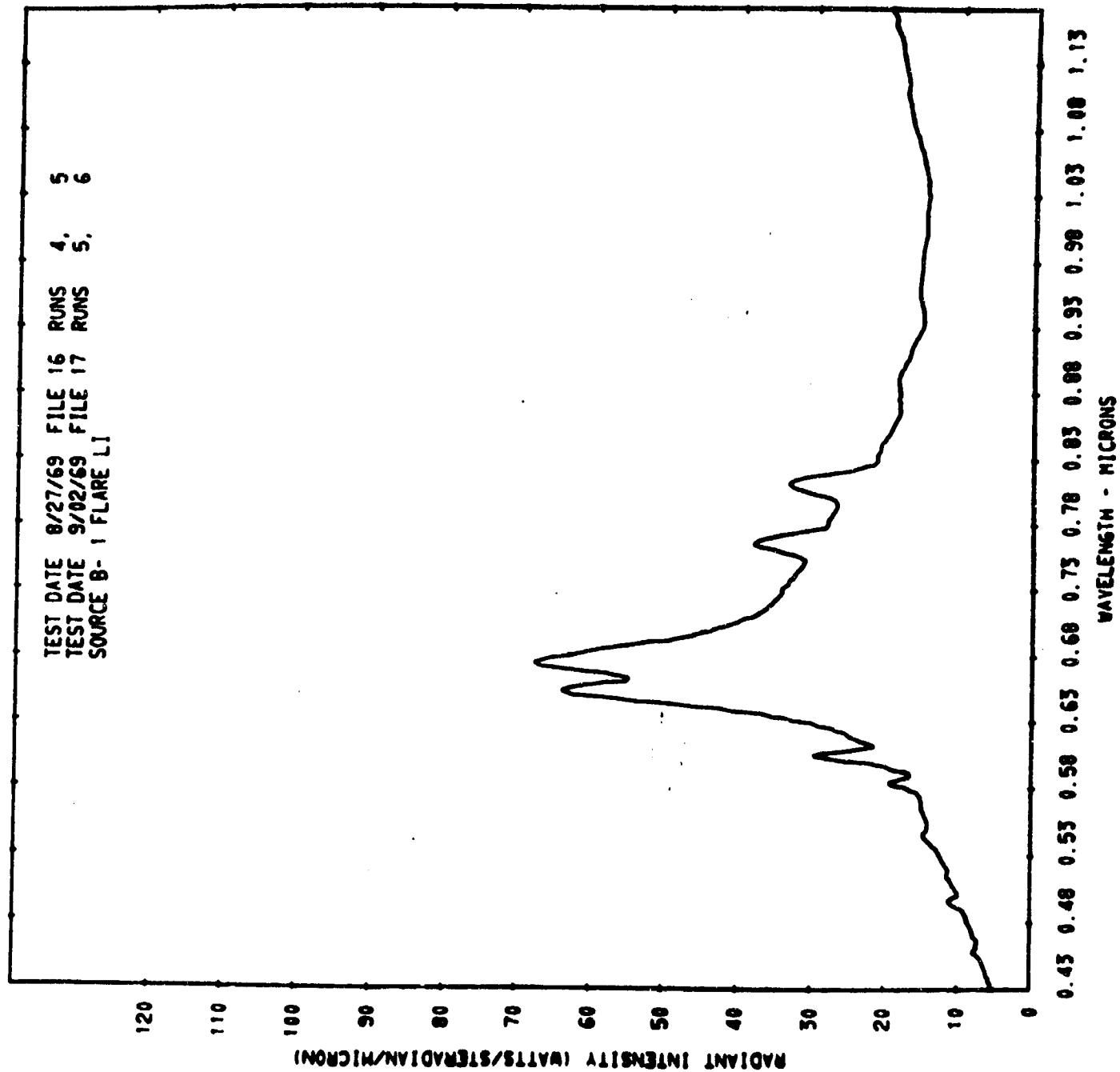
Finally, much work needs to be done to refine and extend these measurements but for the first time a coherent body of quantitative data on these flames has been created.
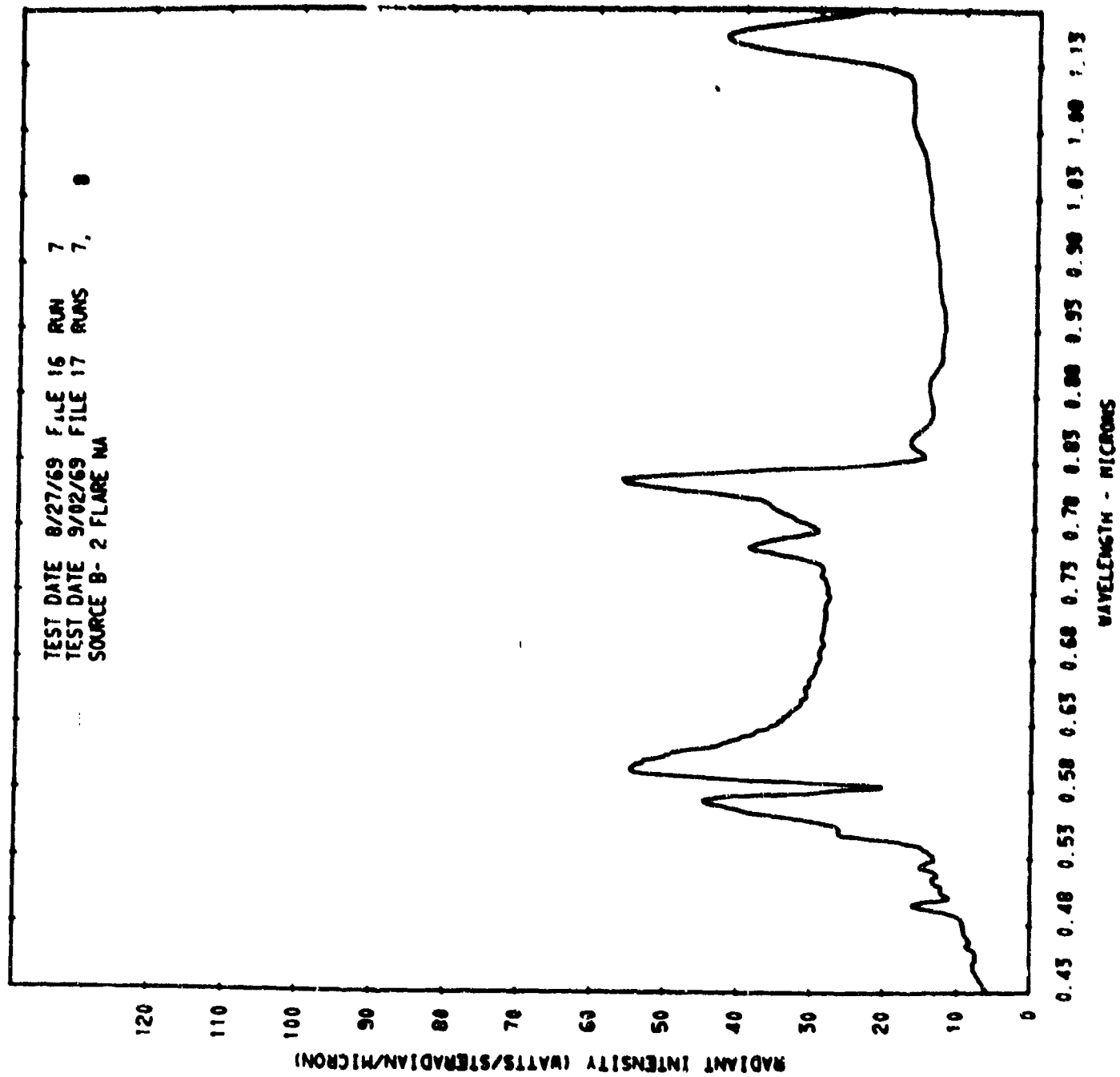
1. Blunt, R. M., "Processes Occurring in Pyrotechnic Flames," Contract N164-10520, U. S. Naval Ammunition Depot, Crane, Indiana, as RDTR No. 35, April 1966.

2. Blunt, R. M., "Production of Colored Flames with Air and Water Reactive Materials," Contract N164-11111, U. S. Naval Ammunition Depot, Crane, Indiana, as RDTR No. 20, June 1966.

3. Blunt, R. M., "Evaluation of Processes Occurring in Pyrotechnic Flames," Contract N164-11171, U. S. Naval Ammunition Depot, Crane, Indiana, as RDTR No. 91, March 1967.

4. Blunt, R. M., "Spectroscopic Studies of Metal-Oxidant Combinations," U. S. Naval Ammunition Depot, Crane, Indiana, as RDTR No. 126, March 1968.

5. Blunt, R. M., "Gelled Illuminant Compositions for Aerial Launch," U. S. Naval Ammunition Depot, as RDTR 116, May 1968.

6. Strong, H. M. and F. P. Bundy, "Measurement of Temperatures in Flames of Complex Structure, etc." Jnl. Applied Physics, 25, No. 12, (1954), pp. 1521-37. Also see J. App. Physics, 22, 1069, (1951).

PLOTS OF SPECTRAL INTENSITY VS. WAVE LENGTH
RANGE 0.43 MICRON - 1.17 MICRON

ELEMENT	TYPE	FILE 16 RUNS	FILE 17 RUNS
Li	B1	4, 5	5, 6
Na	B2	7	7, 8
K	B3	8, 9	11
Rb	B4	10, 11	101, 102
Cs	B5	101, 102	104, 105
Ca	B6	104	108
Sr	B7	105, 106	109, 110
Ba	B8	107, 108	201, 202
Stoich	B17	305, 306	311
Li	B9	2	204
Na	B10	201, 202	205, 206
K	B11	203	207, 208
Rb	B12	205	209, 210
Cs	B13	207, 208	301, 302
Ca	B14	201	304, 305
Sr	B15	302	306, 307
Ba	B16	303	309
Molal	B18	109, 110	401, 402
Stoich NaClO$_4$	B19	307, 308	403, 404
Molal NaClO$_4$	B20	309, 310	406

TEST DATE 8/27/69 FILE 16 RUNS 4, 5
TEST DATE 9/02/69 FILE 17 RUNS 5, 6
SOURCE B- I FLARE LI

RADIANT INTENSITY (WATTS/STERADIAN/MICRON)

WAVELENGTH - MICRONS

A2

TEST DATE 8/27/69 FILE 16 RUN 7
TEST DATE 9/02/69 FILE 17 RUNS 7, 8
SOURCE B- 2 FLARE NA

WAVELENGTH - MICRONS

0.45 0.48 0.53 0.58 0.63 0.68 0.73 0.78 0.83 0.88 0.93 0.98 1.03 1.08 1.13

RADIANT INTENSITY (WATTS/STERADIAN/MICRON)

0 10 20 30 40 50 60 70 80 90 100 110 120

A3

TEST DATE 8/28/69 FILE 16 RUNS 8. 9
TEST DATE 9/82/69 FILE 17 RUN ::
SOURCE B- 3 FLARE K

RADIANT INTENSITY (WATTS/STERADIAN/MICRON)

WAVELENGTH - MICRONS

A4
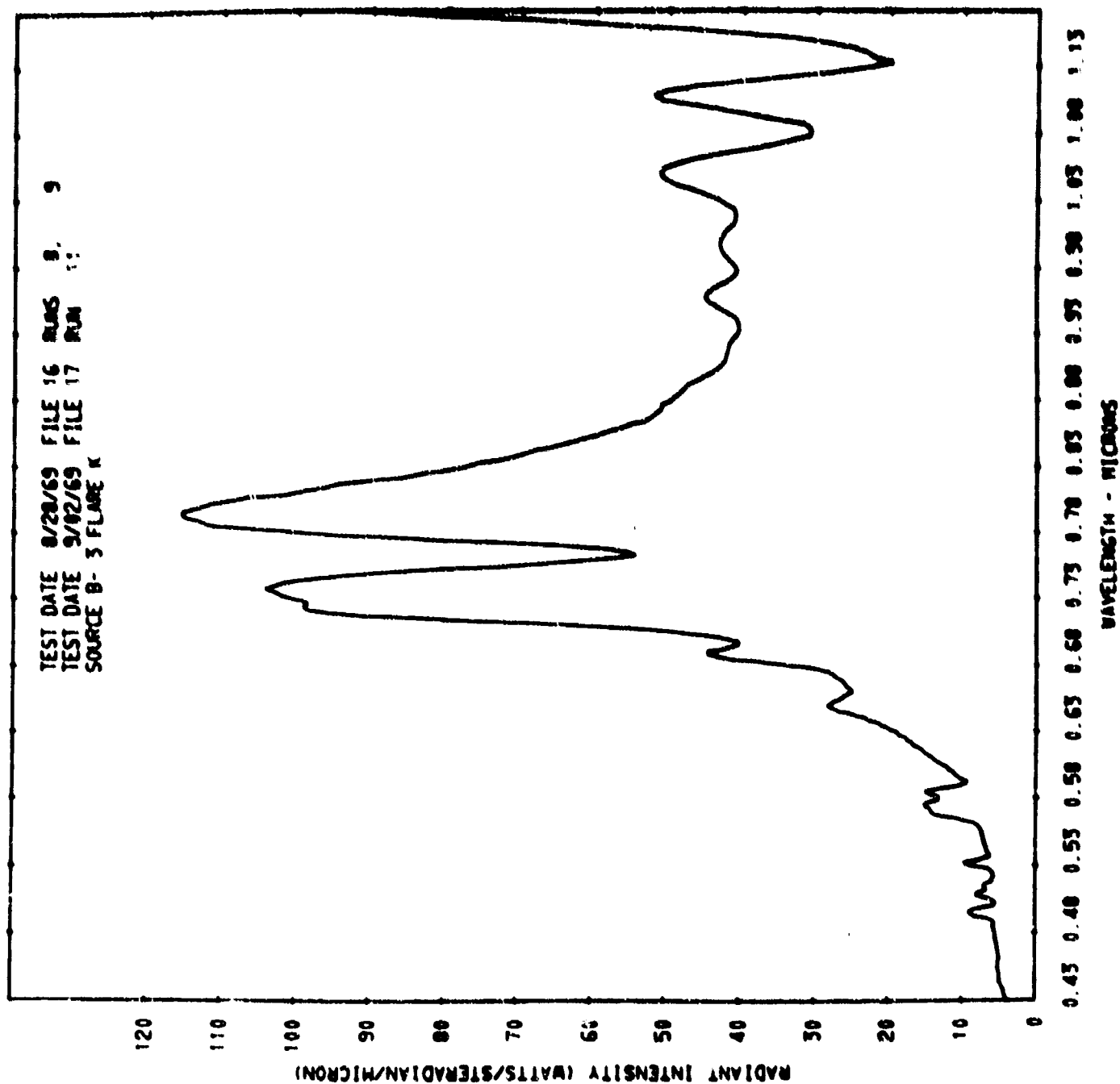
TEST DATE 3/20/69 FILE 16 RUNS 10. 11
TEST DATE 3/62/69 FILE 17 RUNS 101. 102
SOURCE B- 4 FLARE RB

RADIANT INTENSITY (WATTS/STERADIAN/MICRON)

WAVELENGTH - MICRONS

A5
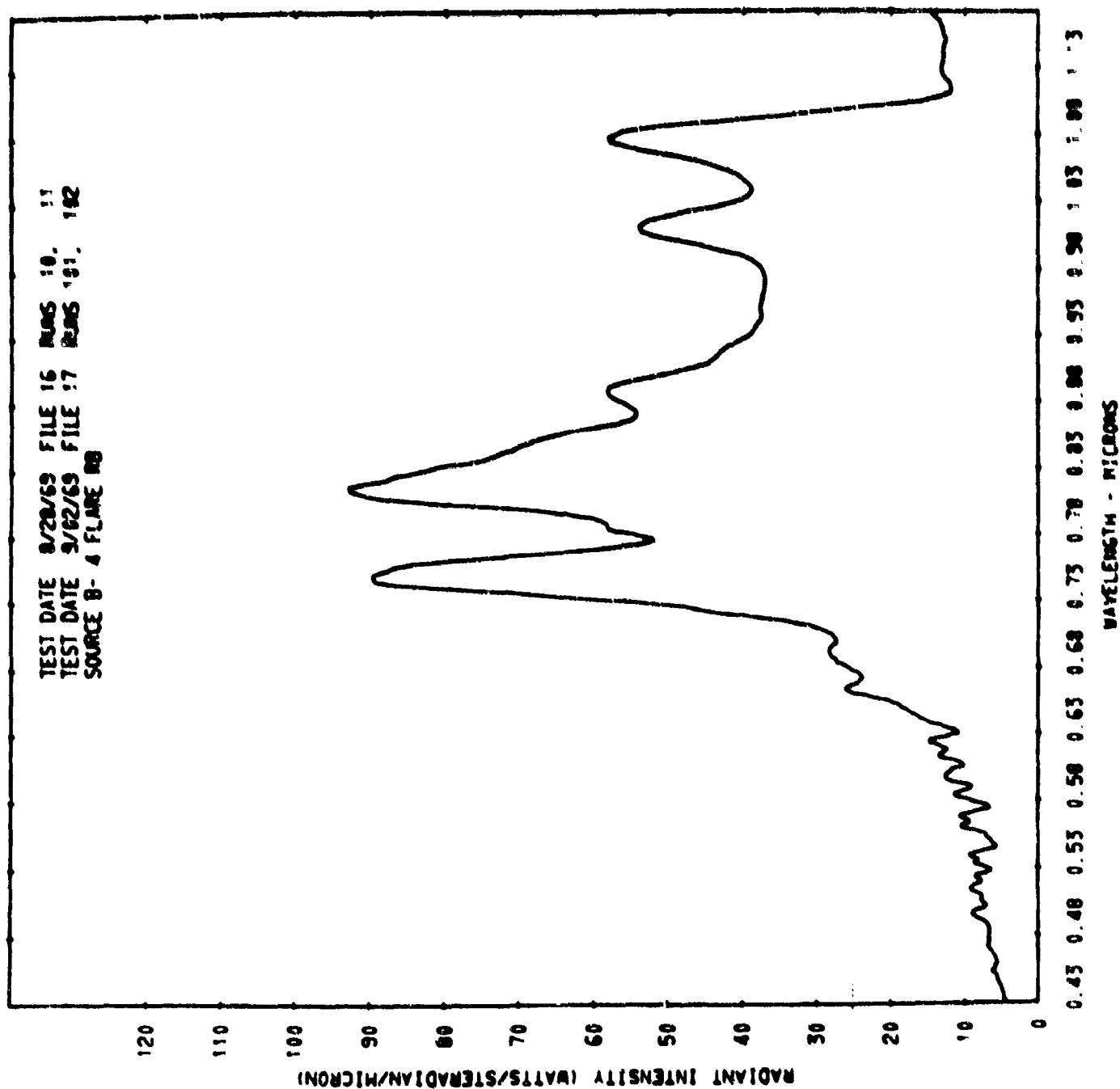
TEST DATE 8/28/69 FILE 16 RUNS 181, 182
TEST DATE 9/82/69 FILE 17 RUNS 184, 185
SOURCE B- 5 FLARE ES

RADIANT INTENSITY (WATTS/STERADIAN/MICRON)

WAVELENGTH - MICRONS

A6
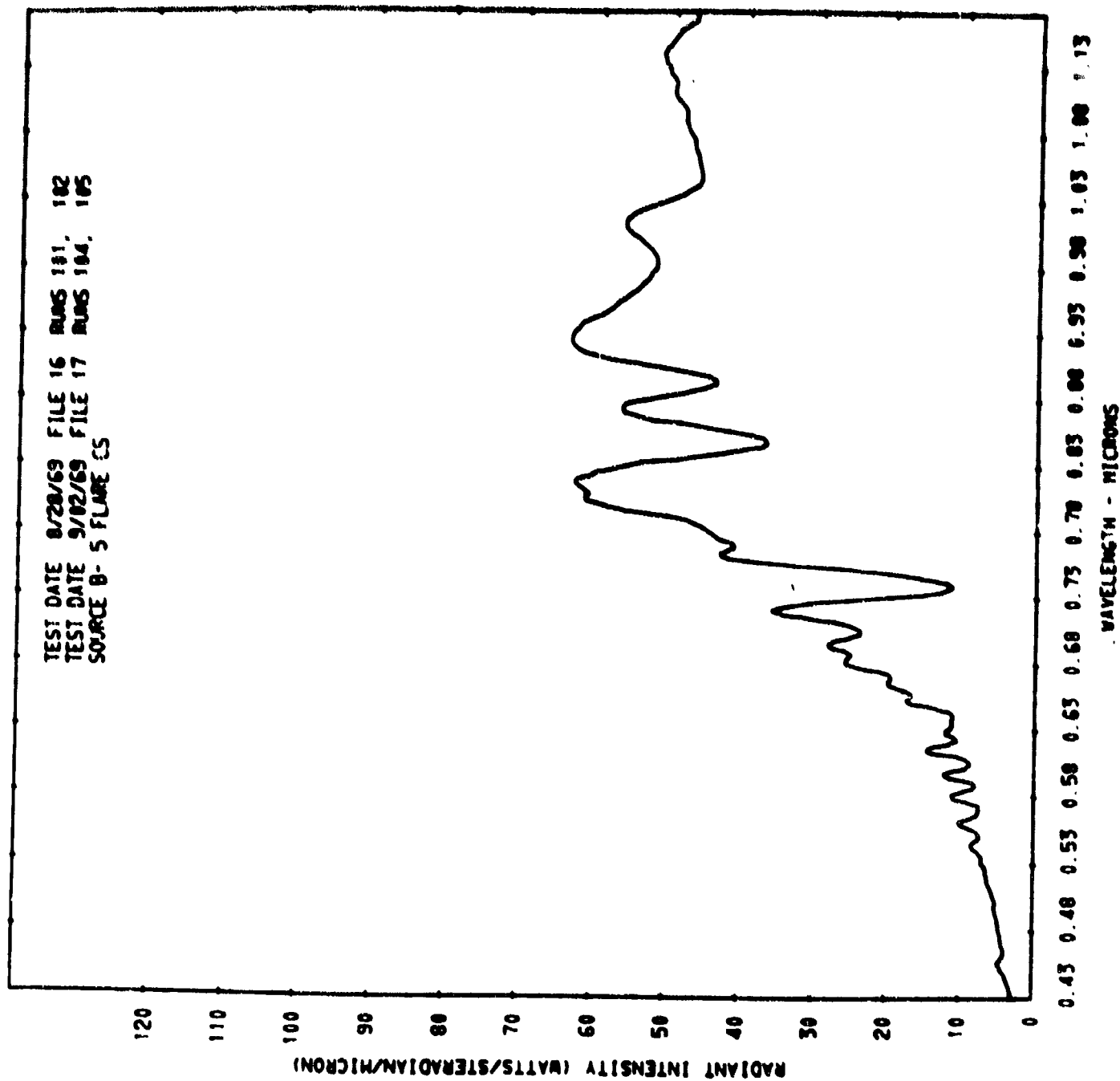
TEST DATE 8/28/69 FILE 16 RUN 104
TEST DATE 9/02/69 FILE 17 RUN 108
SOURCE B- 6 FLARE CA

RADIANT INTENSITY (WATTS/STERADIAN/MICRON)

WAVELENGTH - MICRONS

A7
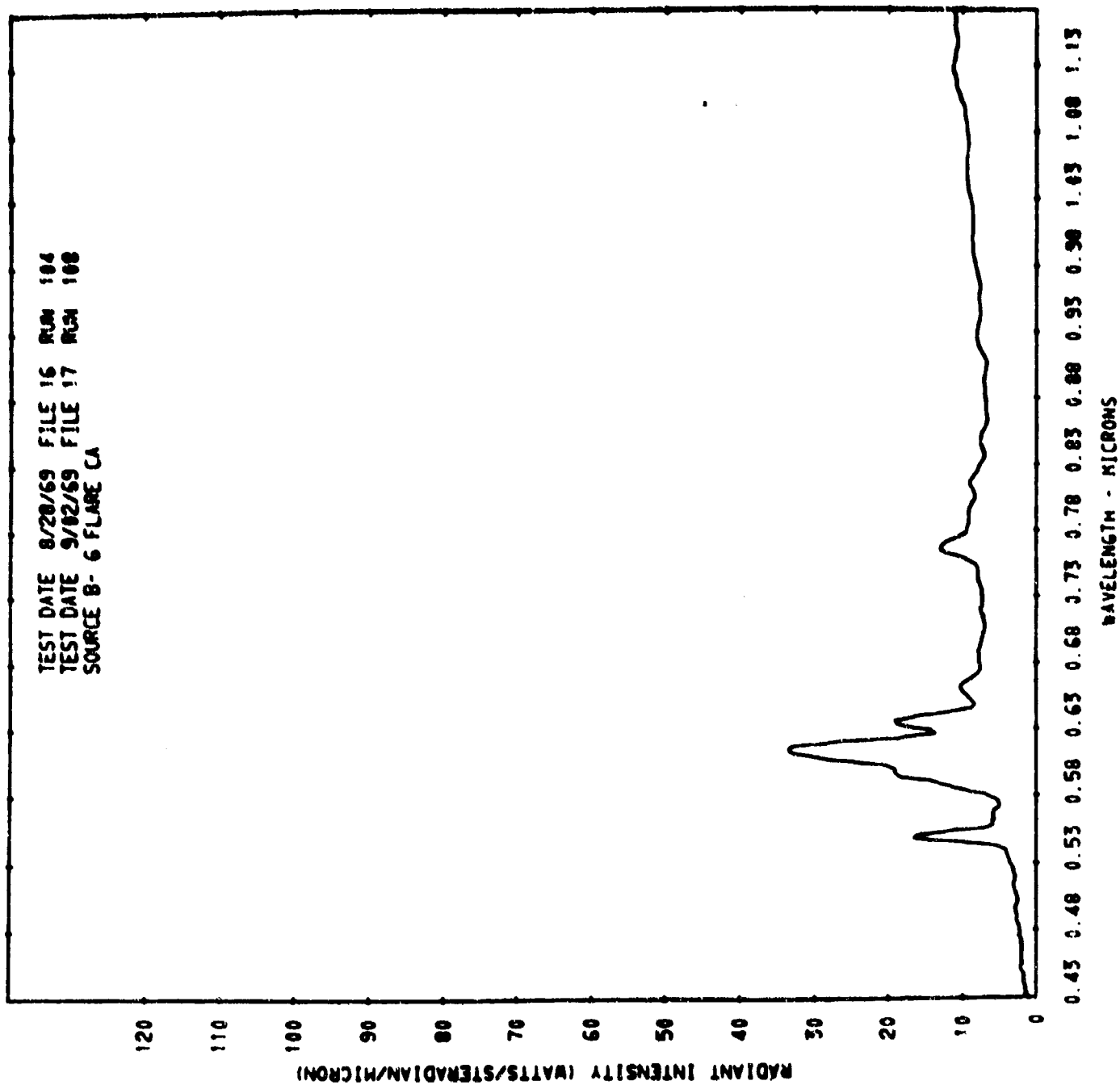
TEST DATE 8/28/69 FILE 16 RUNS 105, 106
TEST DATE 9/02/69 FILE 17 RUNS 109, 110
SOURCE B- 7 FLARE SR

RADIANT INTENSITY (WATTS/STERADIAN/MICRON)

WAVELENGTH - MICRONS

A8

TEST DATE 8/28/69 FILE 16 RUNS 107. 108
TEST DATE 9/03/69 FILE 17 RUNS 201. 202
SOURCE B- 8 FLARE BA

RADIANT INTENSITY (WATTS/STERADIAN/MICRON)

WAVELENGTH - MICRONS
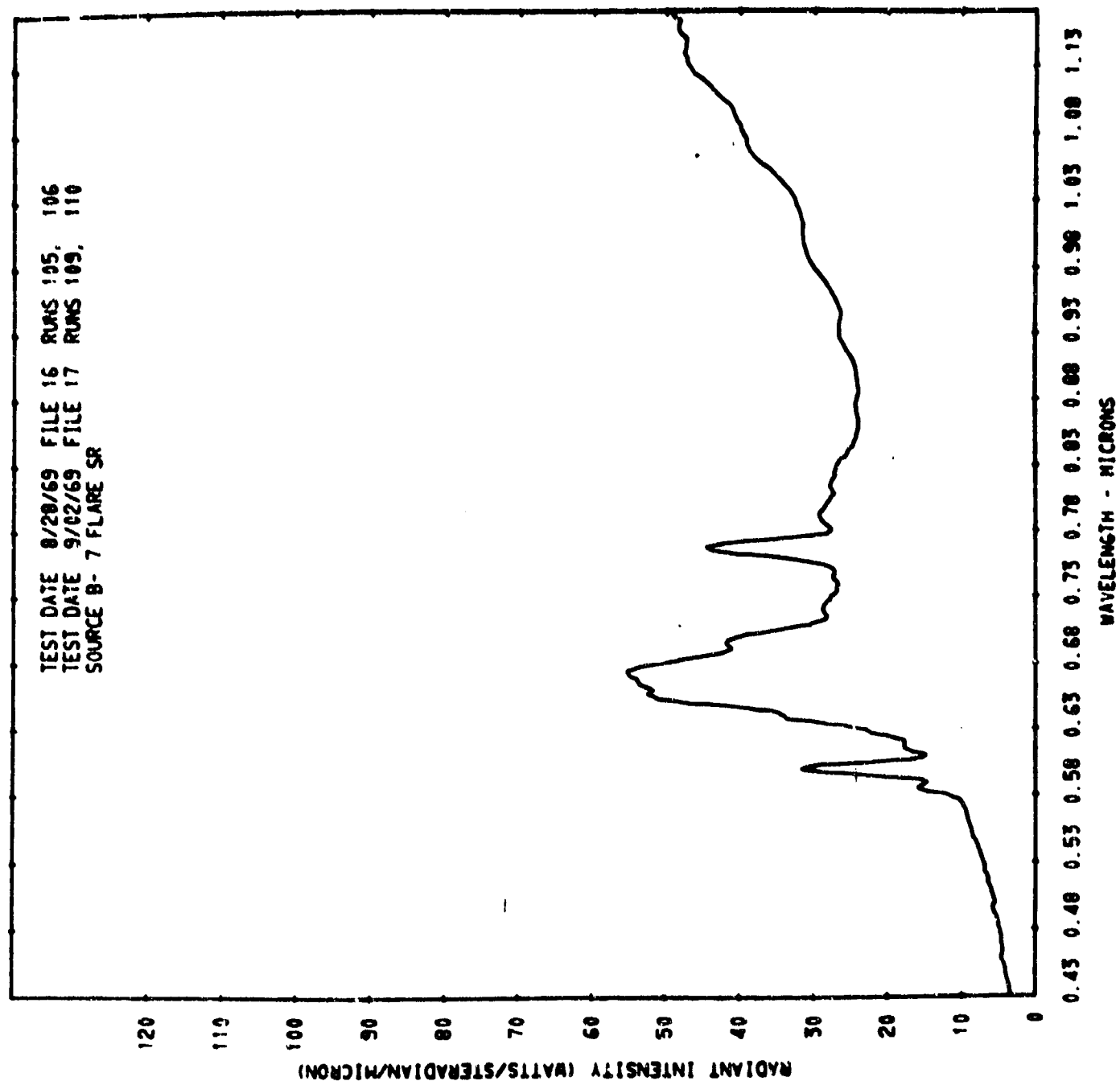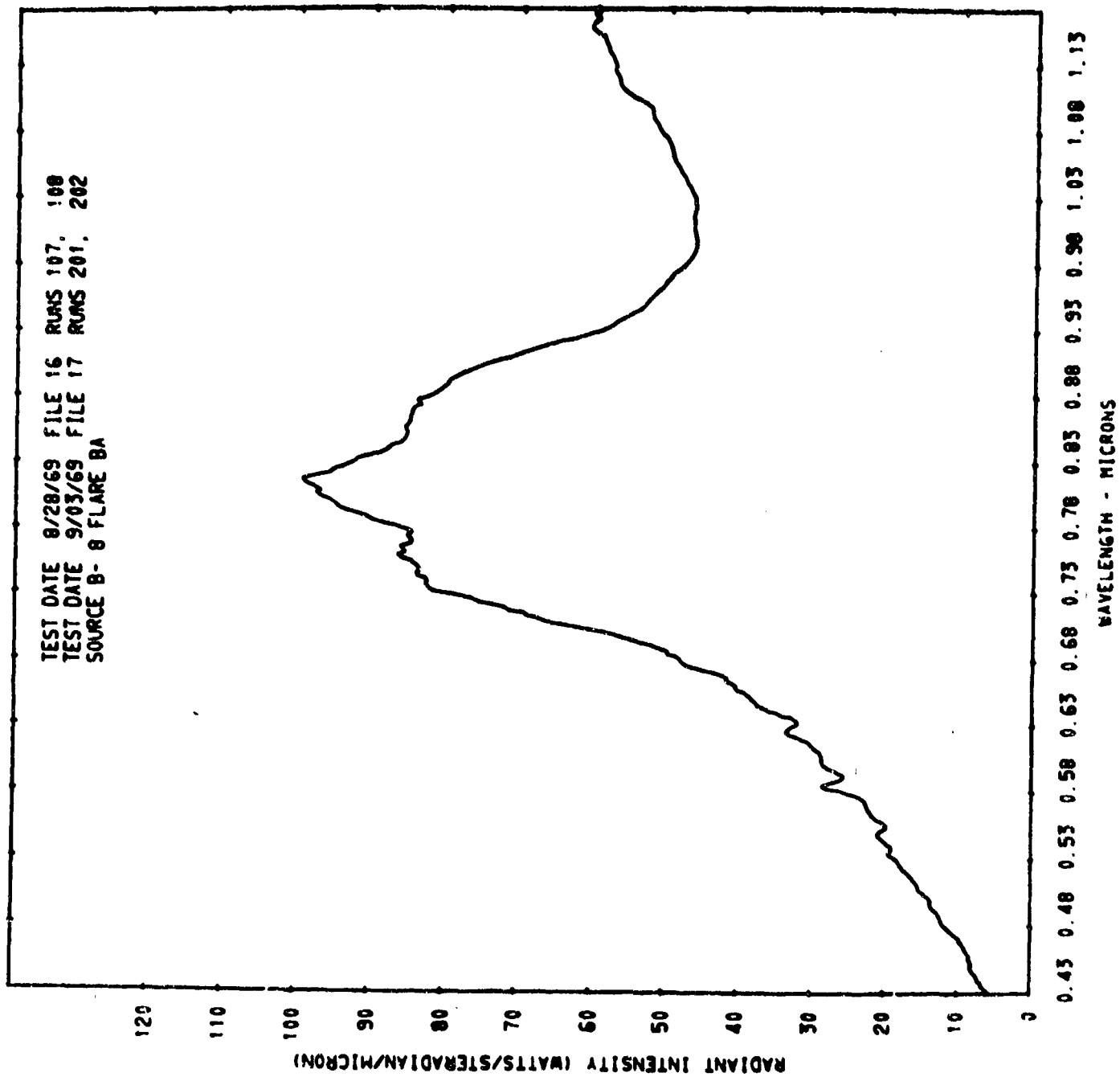
TEST DATE 8/27/69 FILE 16 RUN 2
TEST DATE 9/05/69 FILE 17 RUN 204
SOURCE 8- 9 FLARE LI

RADIANT INTENSITY (WATTS/STERADIAN/MICRON)

WAVELENGTH - MICRONS

0.43 0.48 0.53 0.58 0.63 0.68 0.73 0.78 0.83 0.88 0.93 0.98 1.03 1.08 1.13

A10
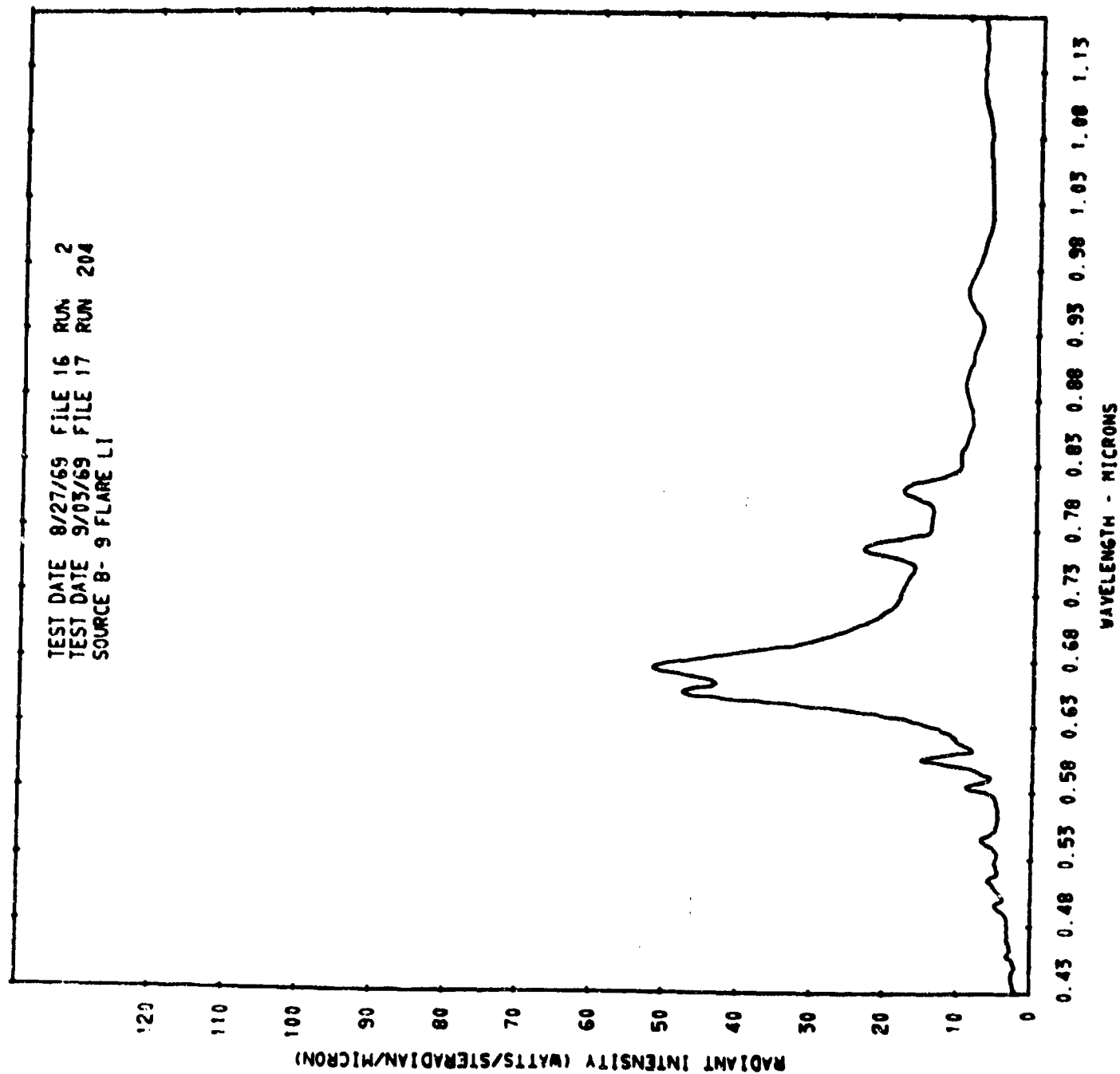
TEST DATE 8/28/69 FILE 16 RUNS 201, 202
TEST DATE 9/05/69 FILE 17 RUNS 205, 206
SOURCE B-10 FLARE NA

WAVELENGTH - MICRONS

RADIANT INTENSITY (WATTS/STERADIAN/MICRON)

A11
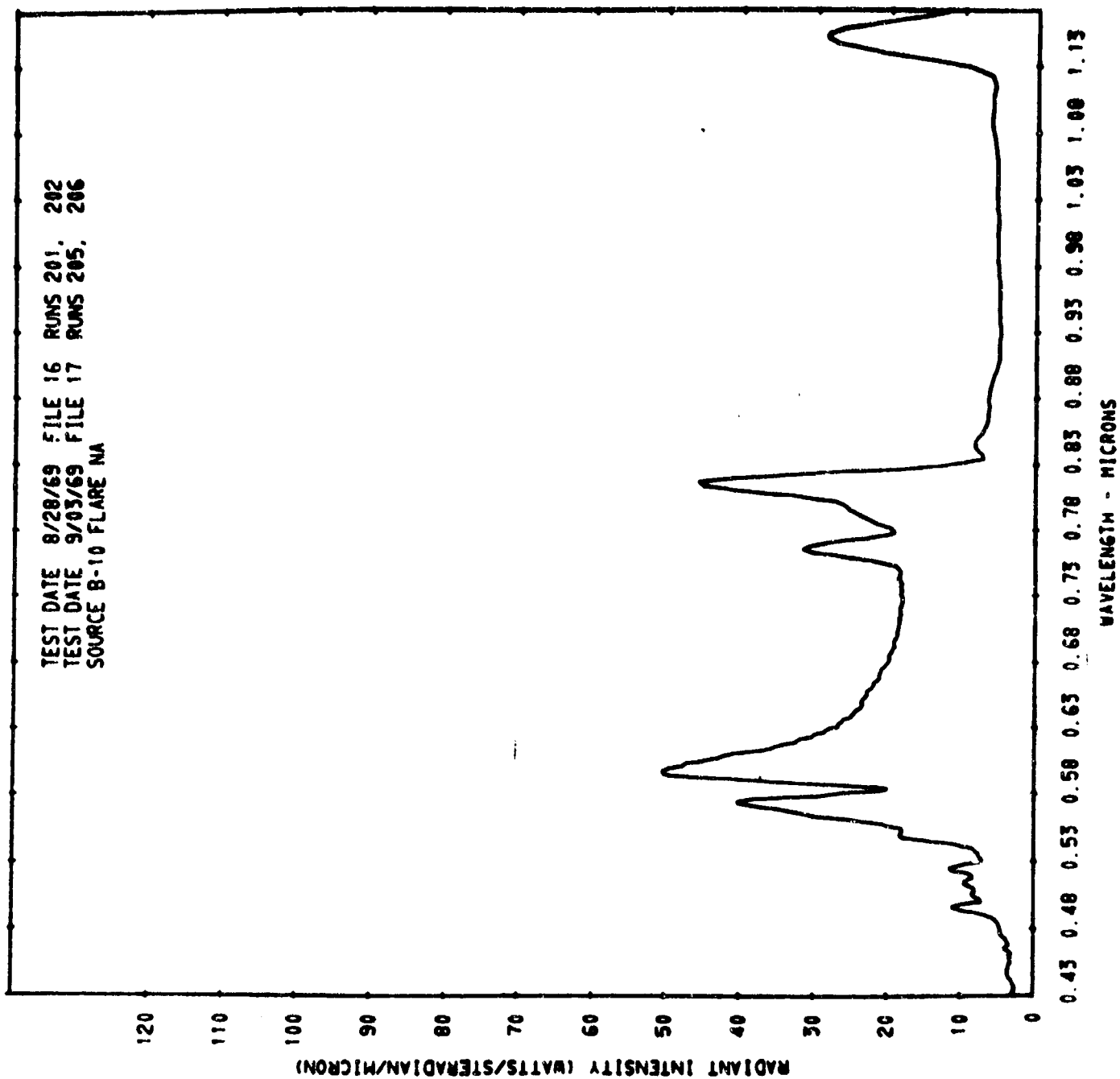
TEST DATE 8/28/69 FILE 16 RUN 203
TEST DATE 9/03/69 FILE 17 RUNS 207. 208
SOURCE B-11 FLARE K

RADIANT INTENSITY (WATTS/STERADIAN/MICRON)

WAVELENGTH - MICRONS

A12

RADIANT INTENSITY (WATTS/STERADIAN/MICRON)

TEST DATE 8/28/69 FILE 16 RUN 205
TEST DATE 9/03/69 FILE 17 RUNS 209, 210
SOURCE B-12 FLARE RB

120 110 100 90 80 70 60 50 40 30 20 10 0

0.45 0.48 0.53 0.58 0.63 0.68 0.73 0.78 0.83 0.88 0.93 0.98 1.03 1.08 1.13

WAVELENGTH - MICRONS

A13
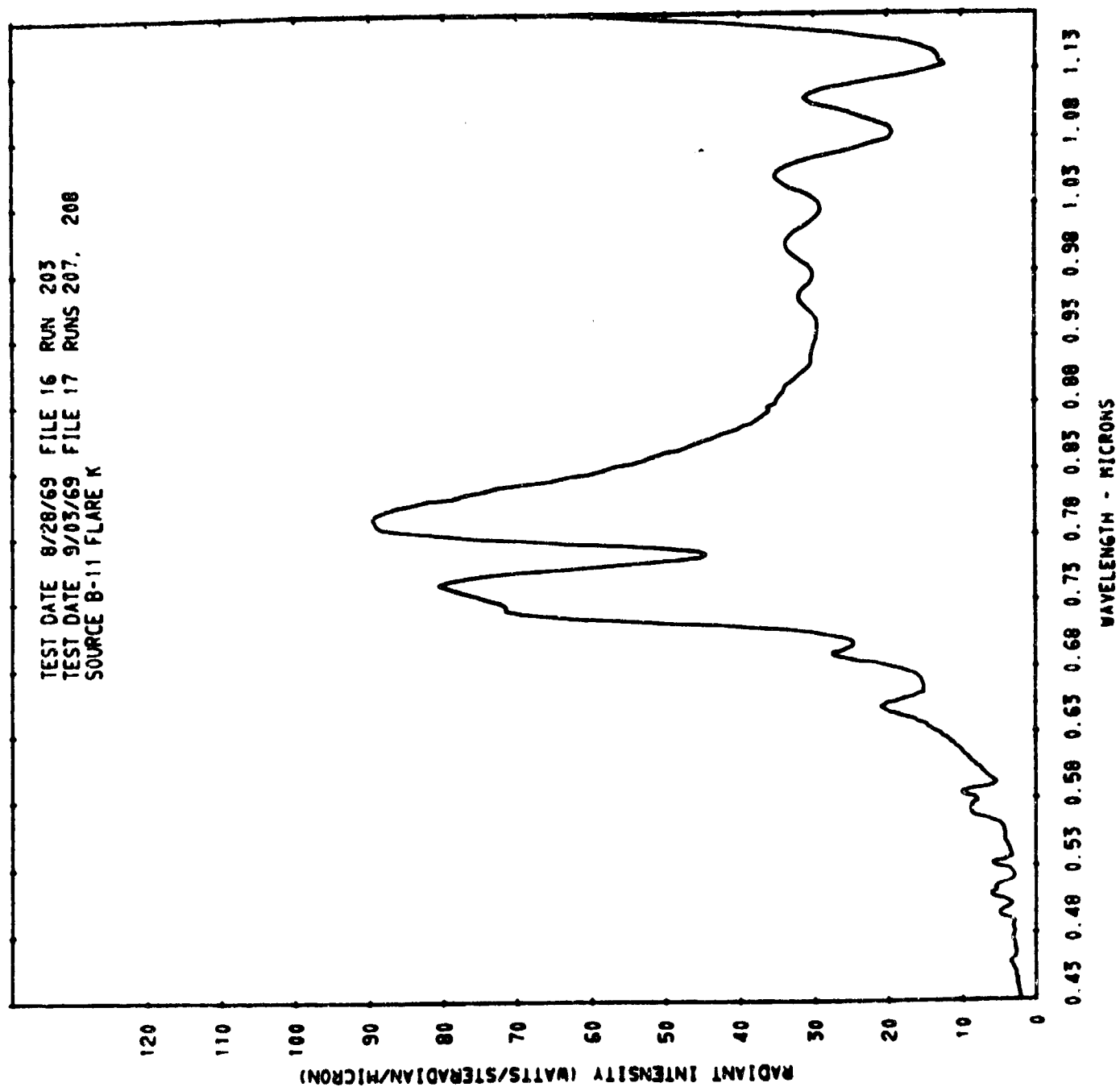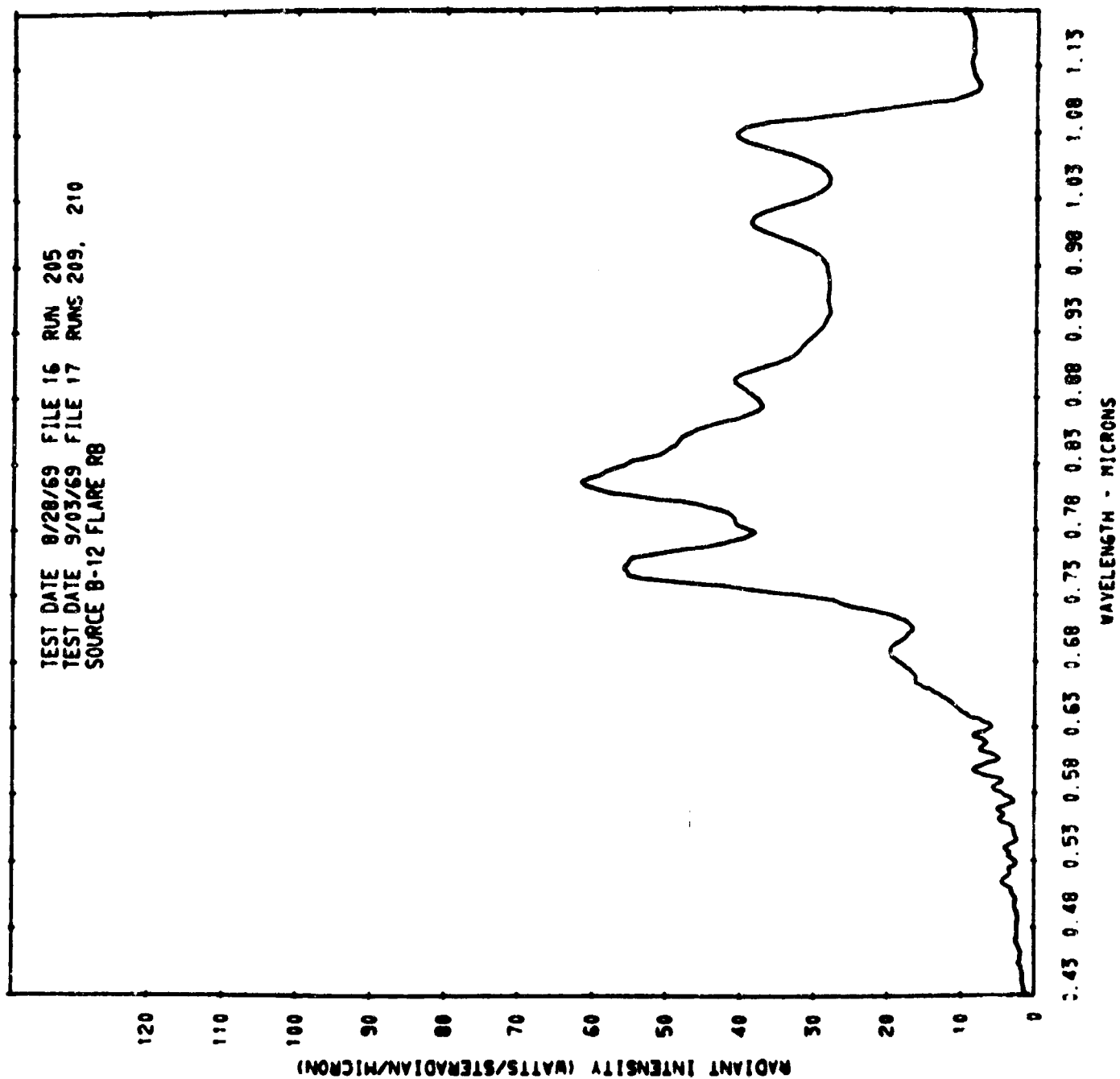
TEST DATE 8/29/69 FILE 16 RUNS 207, 208
TEST DATE 9/03/69 FILE 17 RUNS 301, 302
SOURCE B-13 FLARE CS
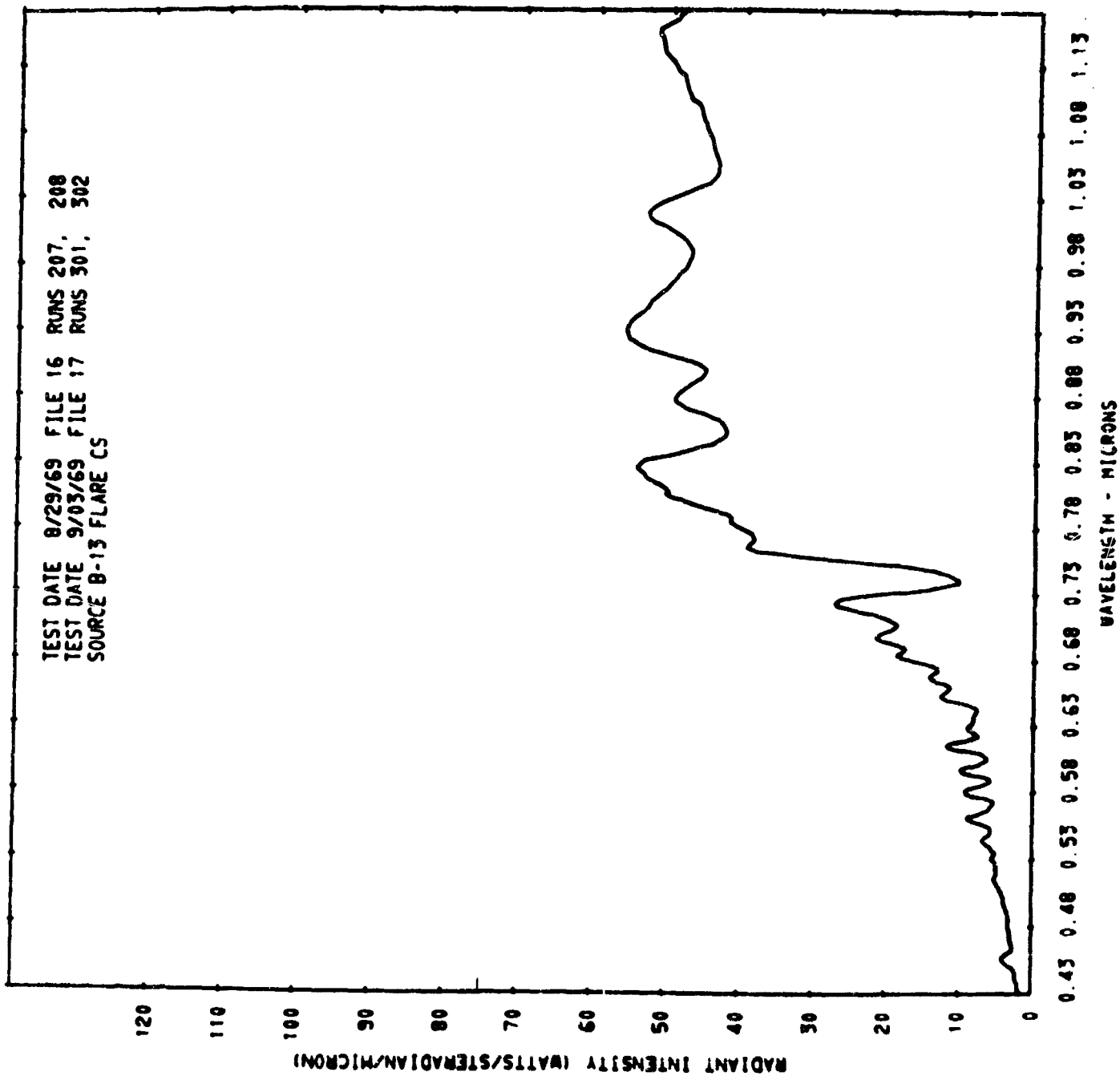
RADIANT INTENSITY (WATTS/STERADIAN/MICRON)

WAVELENGTH - MICRONS

A14

TEST DATE 8/23/69 FILE 16 RUN 213
TEST DATE 9/03/69 FILE 17 RUNS 344, 345
SOURCE B-14 FLARE CA

RADIANT INTENSITY (WATTS/STERADIAN/MICRON)

WAVELENGTH - MICRONS

A15
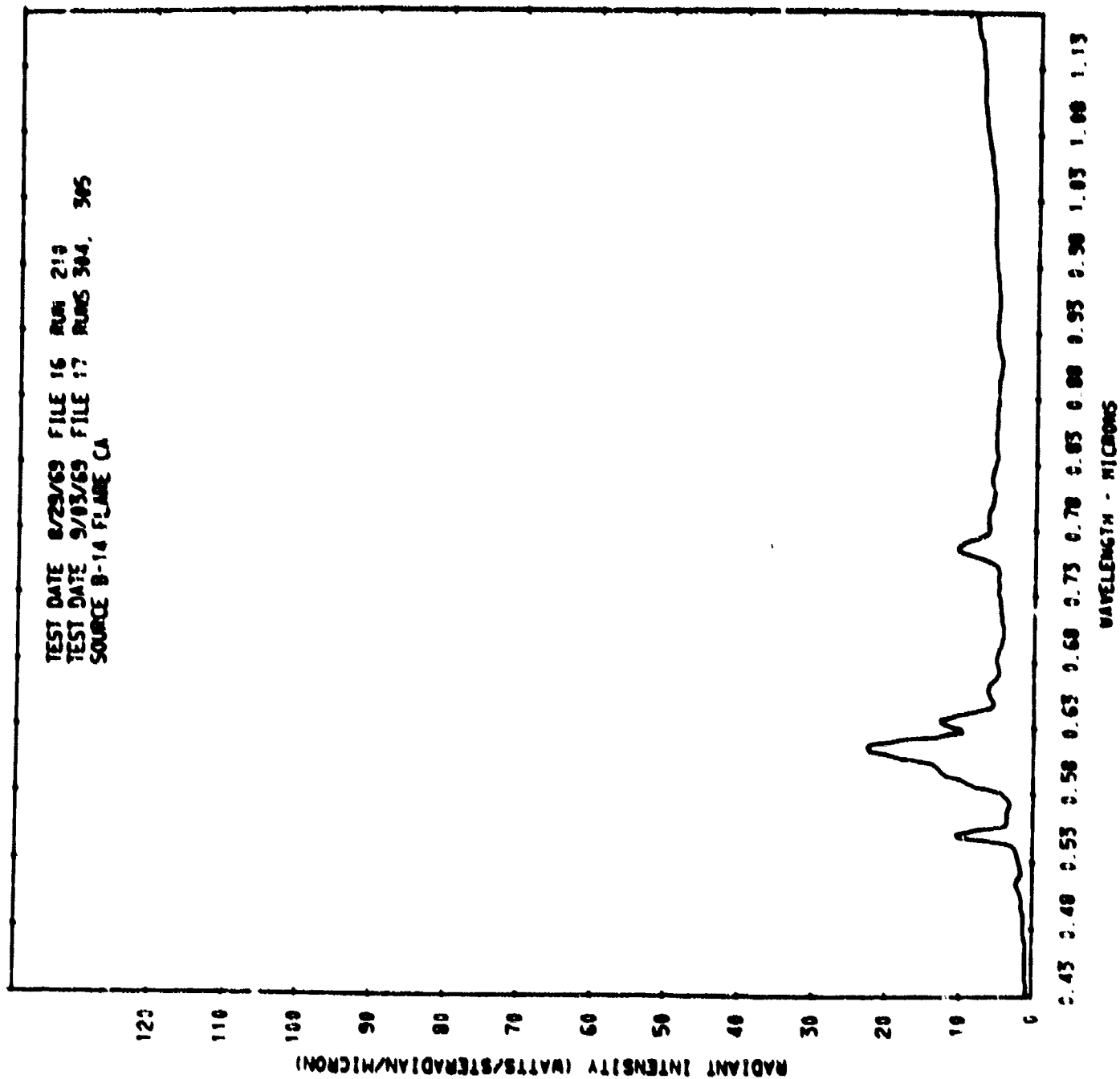
TEST DATE 8/29/69 FILE 16 RUN 382
TEST DATE 9/03/6 FILE 17 RUNS 386. 367
SOURCE B-15 FLARE SR

RADIANT INTENSITY (WATTS/STERADIAN/MICRON)

120 110 100 90 80 70 60 50 40 30 20 10 0

0.48 0.53 0.58 0.63 0.68 0.73 0.78 0.83 0.88 0.93 0.98 1.03 1.08 1.13

WAVELENGTH - MICRONS

A16

RADIANT INTENSITY (WATTS/STERADIAN/MICRON)

120 110 100 90 80 70 60 50 40 30 20 10 0

0.45 0.48 0.53 0.58 0.63 0.68 0.73 0.78 0.83 0.88 0.93 0.98 1.03 1.08 1.13

WAVELENGTH - MICRONS

A18

TEST DATE 8/22/69 FILE 16 RUNS 105, 119
TEST DATE 9/04/69 FILE 17 RUNS 491, 492
SOURCE B-18 FLARE MOLAL MIX

RADIANT INTENSITY (WATTS/STERADIAN/MICRON)

120 110 100 90 80 70 60 50 40 30 20 10 0

0.45 0.48 0.53 0.58 0.63 0.68 0.73 0.78 0.83 0.88 0.93 0.98 1.03 1.08 1.13

WAVELENGTH - MICRONS

A19

TEST DATE 8/29/69 FILE 16 RUNS 307, 308
TEST DATE 9/04/69 FILE 17 RUNS 403, 404.
SOURCE B-19 FLARE NA CLO4

RADIANT INTENSITY (WATTS/STERADIAN/MICRON)

120 110 100 90 80 70 60 50 40 30 20 10 0

0.43 0.48 0.53 0.58 0.63 0.68 0.73 0.78 0.83 0.88 0.93 0.98 1.03 1.08 1.13

WAVELENGTH - MICRONS

A20
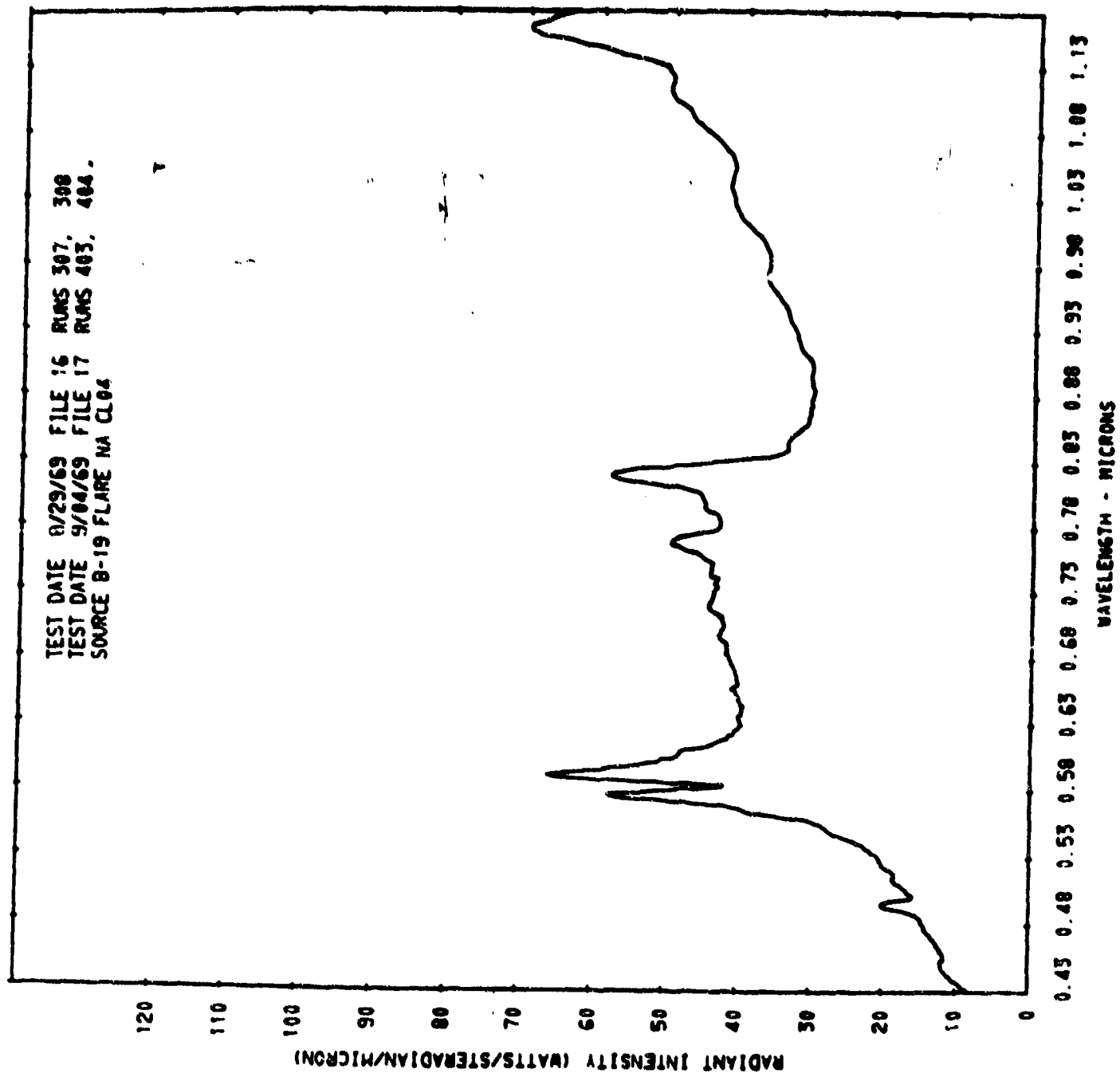
TEST DATE 8/29/69 FILE 16 RUNS 309, 310
TEST DATE 9/04/69 FILE 17 RUN 406
SOURCE B-20 FLARE NA CLO4

RADIANT INTENSITY (WATTS/STERADIAN/MICRON)

WAVELENGTH - MICRONS

0.43 0.48 0.53 0.58 0.63 0.68 0.73 0.78 0.83 0.88 0.93 0.98 1.03 1.08 1.13

A21
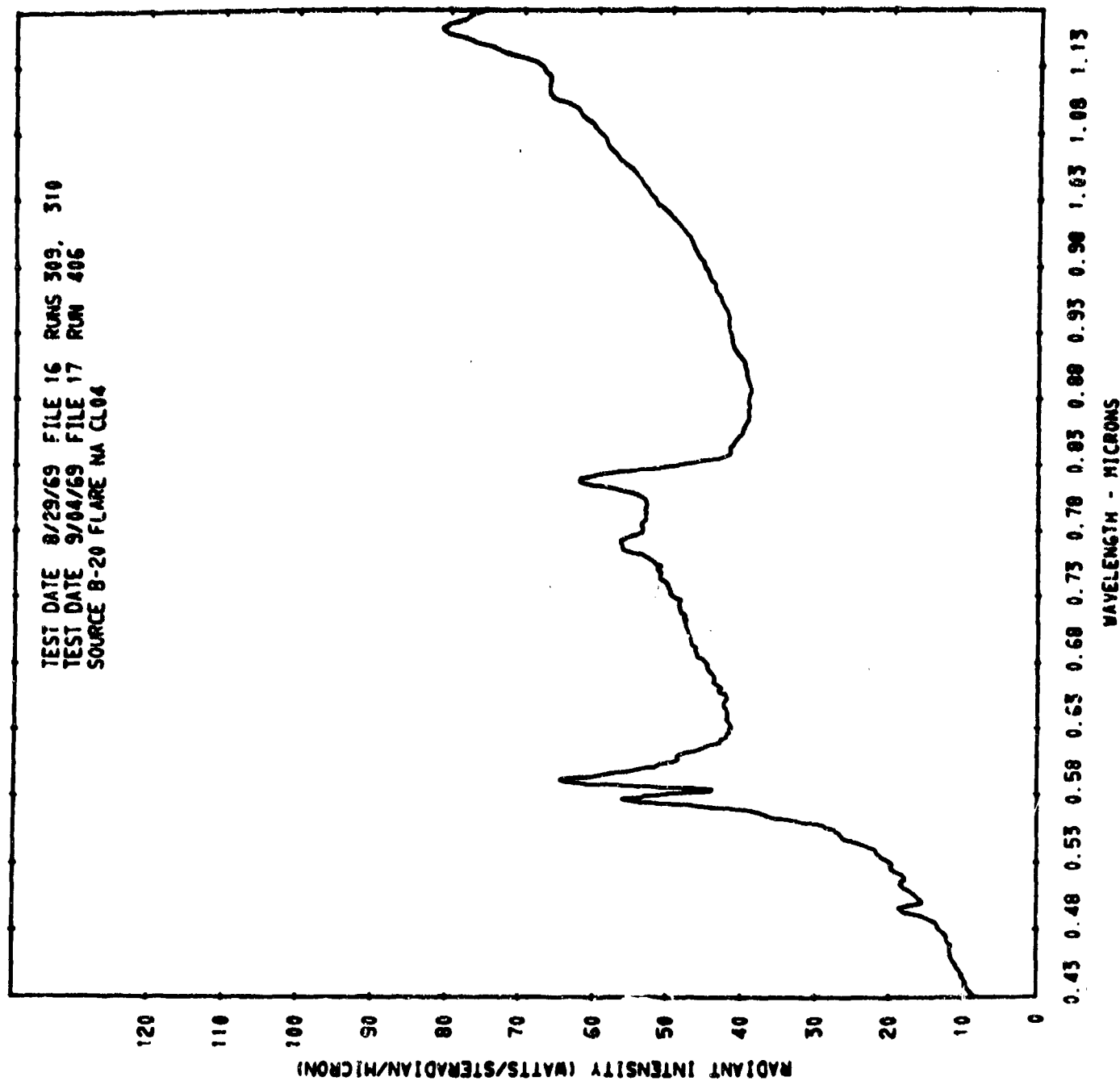
APPENDIX B

ALKALI AND ALKALINE EARTH FLAME SPECTRA
FROM 0.35 MICRON TO 0.90 MICRON

LiNO$_3$

NaNO$_3$

K NO$_3$

RbNO$_3$

CsNO$_3$

Mixed Alkali Nitrates

NaClO$_4$

B1

B2

B3

B4

B5

B17

B19
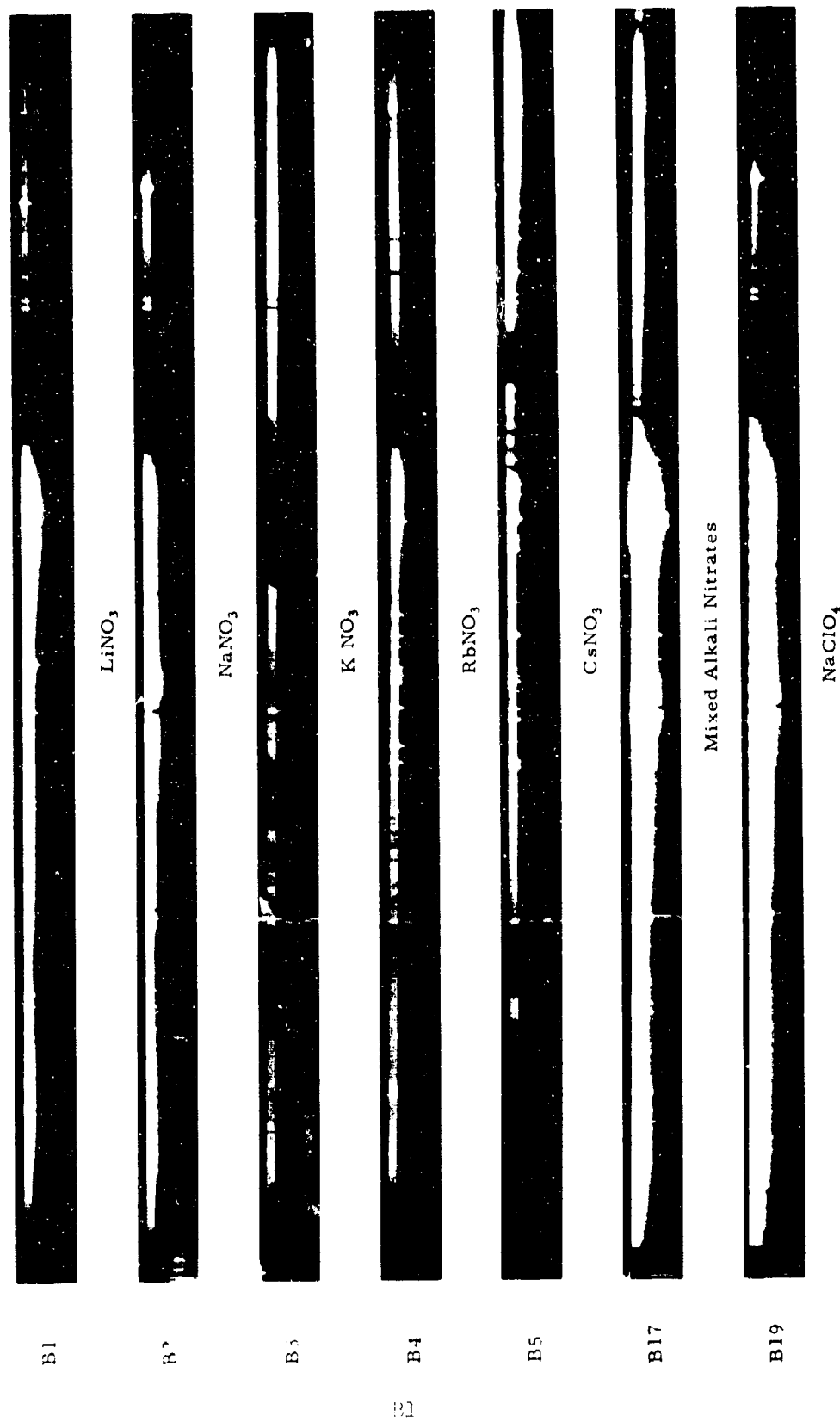
Figure B1.

Grating Spectra of Flames From Stoichiometric Alkali Flare Compositions

LiNO₃

NaNO₃

K NO₃

RbNO₃

CsNO₃

Mixed Alkali Nitrates

NaClO₄

Figure B2

Grating Spectra of Flames From Alkali Flare Compositions with Constant Ratio
1.0 Mol Magnesium to 1.77 Mol Oxygen

Ca (NO₃)₂ (1)

Sr (NO₃)₂ (2)

Ba (NO₃)₂ (3)

Ca (ClO₃)₂ (4)

Sr (ClO₃)₂ (5)

Ba (ClO₃)₂ (6)

Figure 22

Grating Spectra of Flames From Alkaline Earth Flare Compositions that are Stoichiometric (1-3) or Constant Ratio of 1.0 Mol Magnesium to 1.0 Oxygen (4-6)

APPENDIX C

(Bound Separately Because of Page Size)

Explanation of entries in the following tabulation is presented here to aid the reader in correctly interpreting the values.

1) Summary Heading Pages.

Lines 1 through 15 briefly describe the test conditions and identify the flare. The energy content of the mix is calculated by standard procedures, assuming that the end products are magnesium oxide, nitrogen and the cation element.
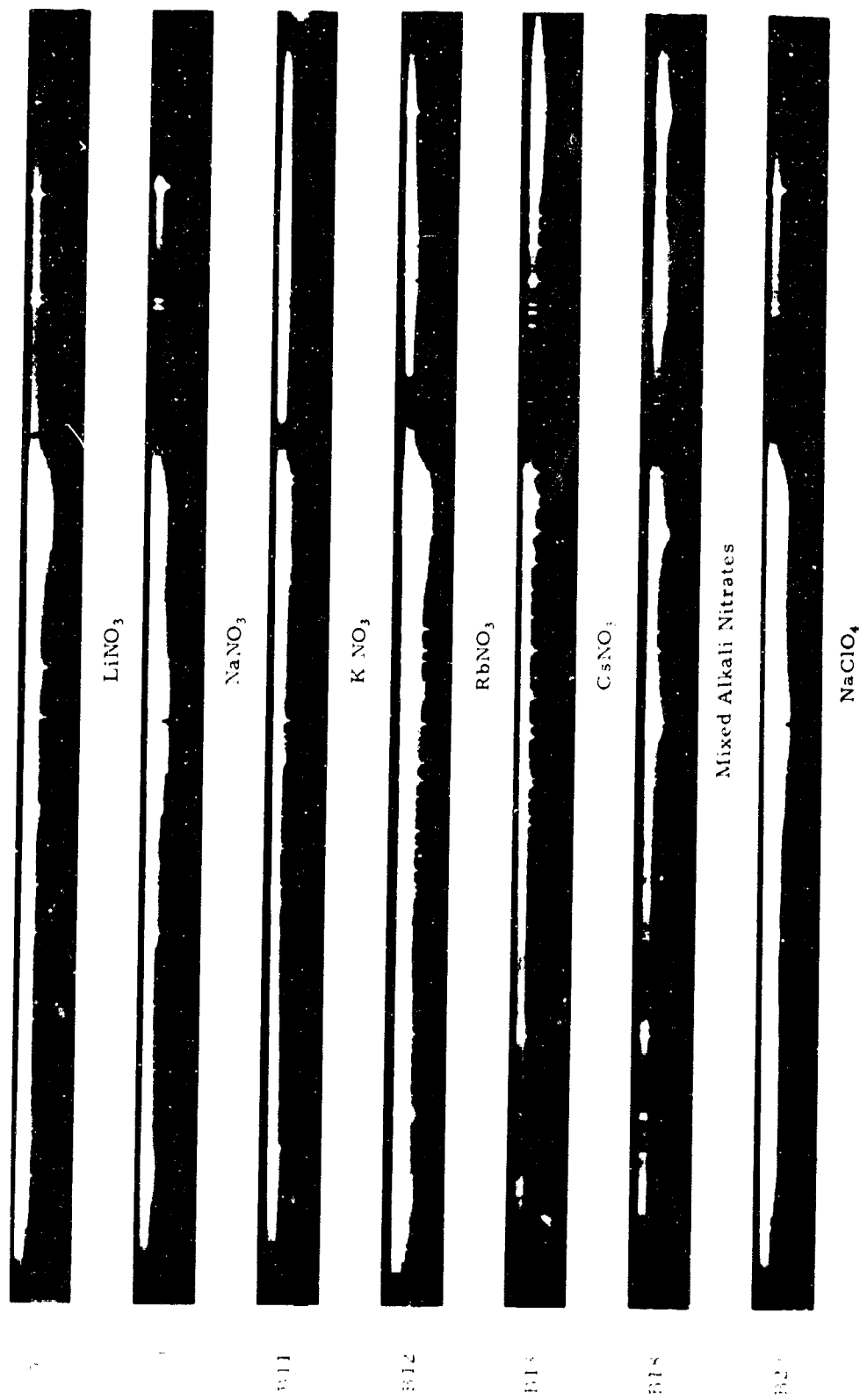
The derivation of Lines 1" and 18 is obviously from the observed time of burn and the values in Line 15.

Line 20 results from the numerical integration of the data tabulated as Column 2, watt ster^{-1} micron^{-1} over the range 0.43-1.171 microns.

Line 21 is calculated by multiplying Line 20 by 4π to represent a spherical emitter, by the burning time in seconds and dividing by the flare weight in grams.

Line 22 is obtained by forming the product of the values in Column 2 with the spectral luminous efficacy (see U.S.A. Standard, "Nomenclature and Definitions for Illuminating Engineering," RP-16, Aug. 16, 1967, pg. 8 pps. 3.7-3.8) values in lumens watt^{-1} at corresponding wavelengths (the resultant product of which is given in Column 6) and numerically integrating the result.

Line 23 is obtained by a) finding the product of Line 22 by 4π times the burning time divided by the composition weight in grams, and b) by finding the product of Line 22 by the burning time in seconds divided by the composition weight in grams, i.e., candela secs gm^{-1}, since 1 lumen ster^{-1} is 1 candela, by definition.

Line 24 is the result of dividing Line 23 (a), lumen secs gm^{-1} by the value of watt seconds gm^{-1} in Line 15 and is a true measure of the luminous efficacy of the area of the flame that was measured, i.e., 4.5 square millimeters.

Line 25-27 values are derived by the usual calculations from the spectral power distribution in Column 2. For details of these computations, see any good text on colorimetry, e.g., "Principles of Illumination," H. Cotton, Wiley, 1), pgs. 186-197. The values quoted define the excitation purity a . color of the luminous radiation from the flames.

Line 30-31 values are obtained by solving Wien's Law for temperature and using the values in Column 2 at the wavelengths given in Line 30-31 to compute the corresponding brightness temperatures for an assumed emissivity of 1.

Line 32 values are the result of finding the ratio between the intensities as computed by Wien's Law at two different wavelengths and solving this expression for the temperature. If the emissivity is not a function of temperature or wavelength, it need not be known for this method to give a true temperature value.

2) Column Contents.

Column 1 gives the wavelength in microns at which the values shown in Columns 2 through 8 apply.

Column 2 gives the radiant intensity in watts steradian^{-1} micron^{-1} computed from the actual measurements of the flame radiation and is the basis of the values in Columns 3 through 8.

Column 3 values are obtained by dividing those in Column 2 by the largest value in Column 2.

Column 4 values represent the area under the curve of spectral radiant flux from the origin at 0.43 micron up to any given tabular entry. They may be used to find the net flux between any two wavelengths.

Column 6 values are the product of those in Column 2 and the spectral luminous efficiency, to create the visible power distribution, which is finally multiplied by 680 lumens watt^{-1} to obtain the value printed at each wavelength.

Column 7 values are analogous to those in Column 4, for luminous flux.

APPENDIX D
EXPERIMENTAL DETAILS

A brief description of the equipment and procedures used to obtain the data is believed to be desirable in order that other investigators may make their own assessment of the results.

The spectra radiated during the combustion of various oxidizers and magnesium flares pressed in 1¼" (33 mm) i.d. fish-paper tubes have been recorded at ambient air pressures which range from 1.0 torr to 760 torr. The spectra of the Mg-NaNO$_3$ candles which were burned at various ambient pressures were recorded with a Perkin-Elmer Model 108 scanning spectrometer operating at about 3 scans per second. The energy transmitted through the spectrometer was detected by an RCA Type 7102 photomultiplier with an S-1 photocathode operated at 1250 volts D. C. from a Type 2K10 Power Designs supply, regulated to 2×10^{-3} percent. This detector sees radiation that has been mechanically chopped at 5400 herz for amplification by a Princeton Applied Research JB-4 phase lock amplifier. The rectified output voltage from the JB-4 was moni-tored on a "Tektronix" 536-B CRO and simultaneously recorded on a "Precision" 7 track magnetic tape recorder. The recorded analog signal tape was processed by the Data Analysis Section of the DRI Electronics Division by first converting the analog signal to digital form, during which operation the recorded signal was reviewed to eliminate bad data. The resultant digital tape was processed on the Burroughs B-5500 computer to apply factors for slit width of spectrometer, neutral density filter transmission vs wavelength, and overall system response as determined by the standard source input-to-output ratio. At the same time, the data were linearized with respect to wavelength, for convenience in plotting. Factors to convert the corrected signal amplitude, which is now in watts micron^{-1} steradian^{-1}, to lumens steradian^{-1} micron^{-1} (or candela) were then applied and the area under the curves calculated. These areas provided the values of watt ster^{-1} and lumens ster^{-1} which measure the efficacy of the source in the wavelength range that was recorded.

The scanning spectrometer detector output circuitry was later somewhat simplified by the elimination of the 5400 herz chopper and associated lock-in signal amplifier, phase and frequency generating photodiodes, etc., that were installed some years ago, when the experimental work was emphasizing the infrared spectral region. The amplitude of the electrical signal from the photomultiplier detectors in the visible and near-infrared was found to be adequate in magnitude without these extra pieces of equipment and their accompanying complications. The scanning rate of the Perkin-Elmer 108 spectrometer was increased to 16 per second, of which only the scans from short-to-long wavelength was used.

The effective scanning rate was thus 8 per second which is actually an increase of about 5 times in the operating speed of the spectrometer. This would have been too fast for the 5400 herz chopping rate of the old system to sample properly and was another reason for the change to a non-chopped mode of operation. The additional data acquired with the increased scanning speed helps to reduce the random noise level in the averaged signal. It was found that the flint glass prism, which had been used for some time in these studies in the visible region, could be replaced to advantage by calcium fluoride because the glass prism has an excessive dispersion in the shorter wavelength region of the spectrum for the present needs of the program. As a result, the data which exist in the red and near-infrared--from, say, 0.7 to 1.2 micron-- were compressed into a relatively small fraction of the total acquisition time. When the data were reduced by the computer, the non-linearity of the flint glass dispersion curve caused a large number of amplitude values to be read out per micron in the short wavelength region, while approximately one-fourth as many were read out in the 0.8-1.2 micron region. The calcium fluoride prism dispersion is also non-linear, but has a shape in the region of interest that is more favorable in terms of equalizing the number of values read out per wavelength interval. As a consequence of the changes in the apparatus and in the data-taking rate, a new set of calibrations for wavelength vs. time and amplitude vs. spectral radiant intensity were required as well as modifications in the data reduction process. One somewhat unfortunate result was an increase in the time required for conversion of the analog data to digital form. Processing of the analog signal tape was done by the Electronics Division of DRI during this time. They found the work load imposed was interfering with prior commitments and contact was then made with the Environmental Science Services Administration personnel at Boulder, Colorado, to determine how their computing and data handling equipment could be used to assist this study. Discussions were held with the objective of acquainting them with these studies and the problems that are involved in making spectral measurements of flares, and to acquaint us with their requirements as to the form in which our data had to be presented to them. The reduction of the data on the alkali and alkaline earth nitrate oxidizers was done at ESSA.

Some slight changes were made when the series of burns with these latter compositions were studied. All of these tests were made at local ambient atmospheric pressure which is taken to be 630 torr. The flares were carefully positioned so that the same region of the flame from each one was viewed by the spectrometer. The center of this region was located one inch above the end of the flare composition, on the axis of the flare candle. The

area of the flame that was "seen" by the spectrometer, with the fore-optics that were used, was 1.5 times the dimension of the spectrometer entrance slit. That is, if the slit is set for a width of 0.2 mm. the region from which the radiation entering the sprctrometer comes is 0.30 mm. wide. The height of the slit was fixed at 10.0 mm. and thus the height of the region viewed in the flame was 15.0 mm. The accuracy of these dimensions was estimated to be ±6%. Thus, the radiation that has been analyzed in these latter studies comes from a region which is 15 mm. high, 0.3 mm. wide centered 25 mm. above the end of the composition. (Constant settings of the spectrometer entrance and exit slits of 0.2 mm. were used in these studies). Two separate detectors, the RCA 7102 and 6217 photomultipliers, were used in order to better cover the spectral region from approximately 0.45 micron - 1.16 micron, with S - 1 and S - 10 photo cathodes in the 7102 and 6217 respectively. No one photocathode available in a photomultiplier covers this entire region with good response.

Two Bausch and Lomb 1.5 meter grating spectrographs were used to secure time-integrated spectra of these same flares, simultaneously with the spectra recorded from the scanning spectrometer. One spectrogram was taken on Linagraph Shellburst film and covered the wavelength range 0.35-0.7 micron, the limit of useful response from this film. The second spectrograph grating was intended to efficiently cover the same 0.35-0.70 micron span, but it was adjusted to cover the 0.55-0.90 micron region. Focus was not as sharp as that of the visible spectra but was adequate for detection, identification and qualitative intensity estimates. This spectral range was recorded on High Speed Infrared film, the response of which decreases very rapidly at longer wavelengths. The response of these films is shown by the manufacturer's data reproduced in Figures A-1 and A-2.

The exposure to record the 0.35-0.70 micron region was made through a 15 step neutral density wedge at the slit in all cases. The 0.55-0.90 micron records were made through a five-step platinum filter. Most of the film was processed in E. K. Co. Type 448 monobath. The supply was exhausted near the end of the series; none was available locally and processing was thereafter done in E. K. Co. Type H. C. 110, followed by Rapid Liquid Fixer. Some difference may exist in the absolute density produced by these two processing schemes which should be considered when comparing films from different burns. The films from any given burn were both processed in the same developer and are, in that sense, comparable. The more prominent lines and band heads appearing on these negatives were identified and one set of negatives from each flare composition marked with india ink to show them.

The stepwedge density values given in Table A-1 are provided for use in estimating the magnitude of the intensity variations recorded in the spectrograms which are contained in Appendix E.

All of the data were obtained from flares burning inside a chamber of six feet inside length and diameter, through glass windows 3/4 inch thick. The effect of the windows and that of the external system was accounted for by making an over-all system calibration with a 1000 watt quartz-iodine lamp positioned in the chamber at the flare location. The spectral steradiancy produced by this lamp is traceable to the National Bureau of Standards. It must be realized that these radiation measurements are extremely difficult to make with much accuracy. For example, the National Bureau of Standards in discussing their calibration of the type of standard lamp used in these flame studies states that the accuracy they obtain ranges from 8% to 3% in the region from 0.35 - 2.5 micron.[1] Their results were obtained under ideal conditions from precisely controlled sources. It is probable that the current measurements on flames are internally quite comparable; on an absolute basis, the accuracy is relatively poor, but still as good as can be expected under the conditions which prevail in the study of pyrotechnics.

[1]Stair, Ralph, Schneider, Wm. E., Jackson, J. K., "New Standard of Spectral Irradiance," Applied Optics, 2, 1151, 1963.
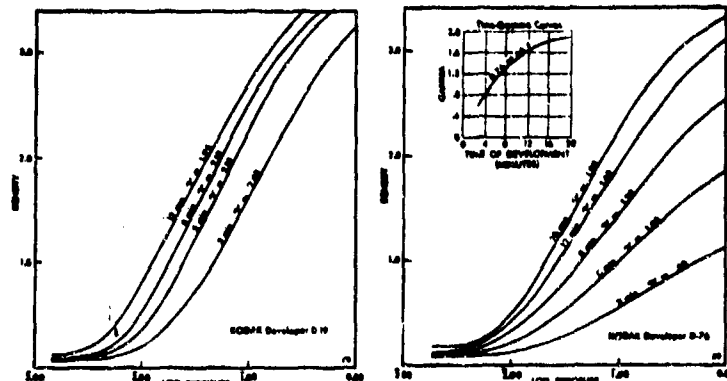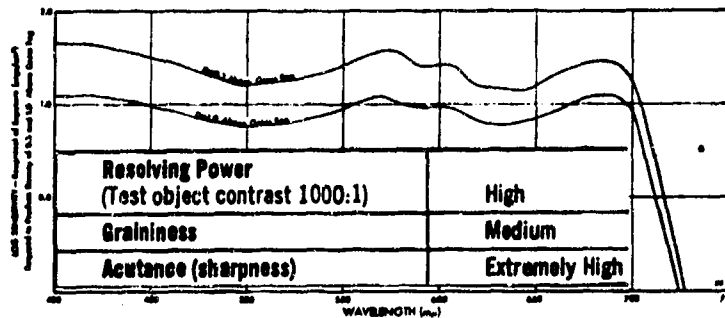
LINAGRAPH SHELLBURST FILM PROPERTIES

Base: ESTAR, 0.004-inch polyester (polyethylene terephthalate plastic). Clear and colorless after processing.

A complete discussion of the physical properties and behavior of this new base is available on request. Ask for KODAK Pamphlet No. Q-34.

Characteristic Curves: KODAK LINAGRAPH Shellburst Film (ESTAR Base). Exposed to daylight illumination for 1/50 second. Developed in KODAK Developers D-19 and D-76 at 68 F (20 C) with continuous agitation.

Spectral Sensitivity Curve: KODAK LINAGRAPH Shellburst Film (ESTAR Base). Developed in KODAK Developer D-19 at 68 F (20 C) for 8 minutes with continuous agitation.

Resolving Power (Test object contrast 1000:1)	High
Graininess	Medium
Acutance (sharpness)	Extremely High

Reciprocity Curve: KODAK LINAGRAPH Shellburst Film (ESTAR Base). Developed in KODAK Developer D-19 at 68 F (20 C) for 8 minutes with continuous agitation.
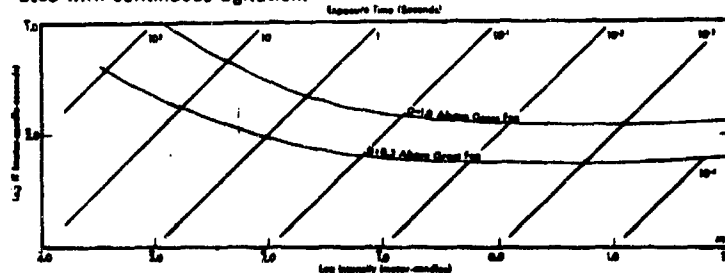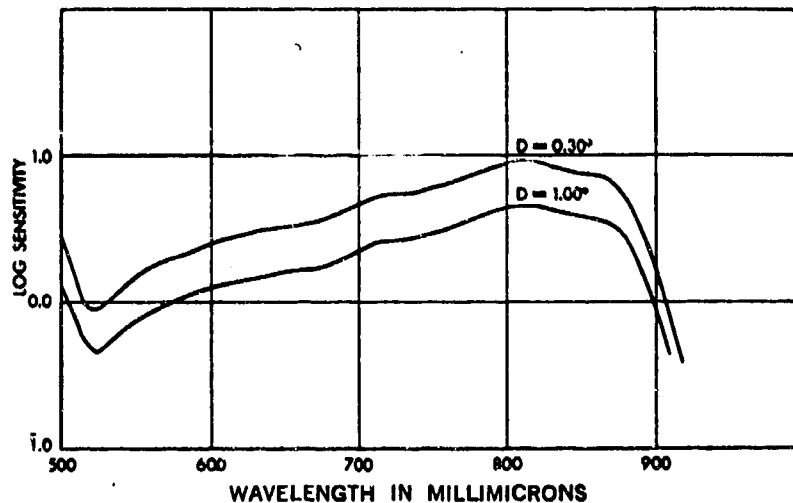
SENSITOMETRIC DATA
Spectral Sensitivity* Curves
Developed 11 minutes in KODAK Developer D-76 at 68 F

WAVELENGTH IN MILLIMICRONS

*Sensitivity = reciprocal of exposure (ergs/cm²) required to produce specified density above density of base plus fog.

Sensitometric Curves: For average product and average processing.
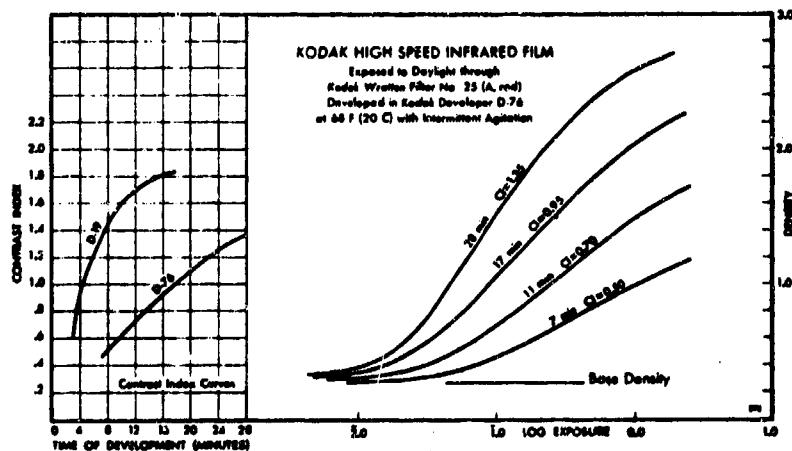
Reciprocity Data:

Exposure Time (seconds)	1/1000	1/100	1/10
Exposure Increase (stops)	+1/3*	none	none

*Increase development to yield 7 percent more contrast.

Forms Available: KODAK High Speed Infrared Film, 16mm—No. HIR 430 (100-ft roll on camera spool for Kodak and other high-speed cameras). KODAK High Speed Infrared Film, 35mm—HIR 421-1 (100-ft roll); 35mm—HIR 417 (100-ft roll on modified No. 10 metal camera spool for Eyemo, DeVry, and similar cameras).

D6

TABLE D-1 FLARE CANDLE COMPOSITION					
Batch No.	Metal	Nitrate %	Magne-sium %	Binder %	Type
0	Na	48.0	48.0	4	Pressure Series
1	Li	46.2	48.8	5	Stoichiometric
2	Na	51.2	43.8	5	"
3	K	55.2	39.8	5	"
4	Rb	63.6	31.4	5	"
5	Cs	69.1	25.9	5	"
6	Ca	54.6	40.4	5	"
7	Sr	60.3	34.7	5	"
8	Ba	64.8	30.2	5	"
17	Li Rb Na Cs K	11.54 12.00 9.17 13.27 10.51	38.51	5	1.0 Mol Mg to 1.77 Moles 0
9	Li	33.4	61.6	5	"
10	Na	38.0	57.0	5	"
11	K	42.0	53.0	5	"

Batch No.	Metal	Nitrate %	Magne- sium %	Binder %	Type
12	Rb	51.0	44.0	5	1.0 Mol Mg to 1.77 Moles O
13	Cs	57.4	37.6	5	"
14	Ca	32.7	62.2	5	"
15	Sr	43.1	51.9	5	"
16	Ba	48.1	46.9	5	"
18	Li K Na Rb Cs	8.34 9.62 6.81 11.03 8.00	51.21	5	Stoichiometric
19	Na	54.8*	40.2	5	Same Sodium Content as 57.38 $Mg-NaNO_3$
20	Na	39.5*	55.52	5	1.0 Mol Mg to 1.77 Moles O

TABLE D-1 CONT'D
FLARE CANDLE COMPOSITION

* Oxidizer is $NaClO_4$, not $NaNO_3$

D8

TABLE D-2

APPROXIMATE STEPWEDGE DENSITIES

Step No.	Platinum Wedge	E. K. Co. Film Wedge
0	0.00	0.06
1	0.74	0.36
2	1.51	0.60
3	2.04	0.84
4	2.75	1.08
5	N.A.	1.31
6	N.A.	1.55
7	N.A.	1.80
8	N.A.	2.03

DOCUMENT CONTROL DATA - R & D

Security classification of title, body of abstract and indexing annotation must be entered when the overall report is classified

1. ORIGINATING ACTIVITY (Corporate author)	2a. REPORT SECURITY CLASSIFICATION
Mechanics Division Denver Research Institute University of Denver Denver, Colorado 80210	UNCLASSIFIED
	2b. GROUP

3. REPORT TITLE

STUDY OF ILLUMINATING FLAMES FROM SOLID REACTANTS

4. DESCRIPTIVE NOTES (Type of report and inclusive dates)

Final Report August 1968 - April 1970

5. AUTHOR(S) (First name, middle initial, last name)

Blunt, Robert M.

6. REPORT DATE	7a. TOTAL NO. OF PAGES	7b. NO. OF REFS
1 June 1970		
8a. CONTRACT OR GRANT NO.	9a. ORIGINATOR'S REPORT NUMBER(S)
AIRTASK NO. A35-532/323/70F17-540-502	Final Report 4178-7003-F
b. PROJECT NO. Work Unit No. 2	
c.	9b. OTHER REPORT NO(S) (Any other numbers that may be assigned this report) RDTR 77
d. N00164-69-C-0036	

10. DISTRIBUTION STATEMENT

Distribution of this document is unlimited.

11. SUPPLEMENTARY NOTES	12. SPONSORING MILITARY ACTIVITY
- - - - - - - - - - - - -	Naval Ammunition Depot Crane, Indiana 47522

13. ABSTRACT

This report summarizes and describes an extensive spectroradiometric study of the radiation produced in the 0.43 micron - 1.17 micron region by flames resulting from the combustion of magnesium with the alkali and alkaline earth nitrates and with sodium perchlorate at an ambient air pressure of 630 torr. Both fuel rich and stoichiometric compositions were studied.

Additional studies were made of the influence of the ambient air pressure on the combustion of a 57% Mg, 38% $NaNO_3$, 5% Laminac composition at ambient air pressure ranging from 760 torr to 1 torr to determine quantitatively the decline in output.

It has been shown that 1) burning rate, radiance and luminance decrease exponentially as the ambient pressure is decreased, and quantitative expressions are derived for these changes, 2) the ratio of visible to total radiation increases as the pressure decreases, 3) sodium perchlorate compositions radiate considerably more in the region 0.8-1.17 micron than sodium nitrate compositions, 4) a central zone of the flame radiates more energy from stoichiometric compositions than from fuel rich compositions, 5) flame temperatures computed from the spectra agree with the theoretical predictions within experimental error, 6) reasonable emissivity value in the region of the D lines can be estimated, 7) the energy radiated in a particular spectral region can be maximized by a proper choice of the oxidizer cation.

	KEY WORDS	LINK A		LINK B		LINK C	
		ROLE	WT	ROLE	WT	ROLE	WT
	Flares						
	Illuminating Flares						
	Signalling Flares						
	Colored Flares						
	Flames						
	Emitters						
	Spectra						
	Luminous Intensity						
	Alkali Metals						

DD FORM 1473 (BACK)

(PAGE 2)